HHS Public Access

Author manuscript

Neuroscience. Author manuscript; available in PMC 2018 June 14.

Published in final edited form as:

Neuroscience. 2017 June 14; 353: 58–75. doi:10.1016/j.neuroscience.2017.03.060.

Group II Metabotropic Glutamate Receptor Interactions with NHERF Scaffold Proteins: Implications for Receptor Localization in Brain

Stefanie L. Ritter-Makinson[1], **Maryse Paquet**[1], **James W. Bogenpohl**[2], **Rachel E. Rodin**[1], **C. Chris Yun**[3], **Edward J. Weinman**[4], **Yoland Smith**[2,5], and **Randy A. Hall**[1]

[1]Department of Pharmacology, Emory University School of Medicine, Atlanta, GA 30322, USA

[2]Yerkes National Primate Research Center, Emory University, Atlanta, GA 30329, USA

[3]Department of Medicine, Division of Digestive Diseases, Emory University School of Medicine, Atlanta, GA 30329

[4]Department of Medicine, University of Maryland School of Medicine, Baltimore, MD 21201, USA

[5]Department of Neurology, Emory University School of Medicine, Atlanta, GA 30322, USA

Abstract

The group II metabotropic glutamate receptors mGluR2 and mGluR3 are key modulators of glutamatergic neurotransmission. In order to identify novel Group II mGluR-interacting partners, we screened the C-termini of mGluR2 and mGluR3 for interactions with an array of PDZ domains. These screens identified the Na+/H+ exchanger regulatory factors 1 and 2 (NHERF-1 & -2) as candidate interacting partners. Follow-up co-immunoprecipitation studies demonstrated that both mGluR2 and mGluR3 can associate with NHERF-1 and NHERF-2 in a cellular context. Functional studies revealed that disruption of PDZ interactions with mGluR2 enhanced receptor signaling to Akt. However, further studies of mGluR2 and mGluR3 signaling in astrocytes in which NHERF expression was reduced by gene knockout (KO) and/or siRNA knockdown techniques revealed that the observed differences in signaling between WT and mutant mGluR2 were likely not due to disruption of interactions with the NHERF proteins. Electron microscopic analyses revealed that Group II mGluRs were primarily expressed in glia and unmyelinated axons in WT, NHERF-1 and NHERF-2 KO mice, but the relative proportion of labeled axons over glial processes was higher in NHERF-2 KO mice than in controls and NHERF-1 KO mice. Interestingly, our anatomical studies also revealed that loss of either NHERF protein results in ventriculomegaly, which may be related to the high incidence of hydrocephaly that has previously been observed in NHERF-1 KO mice. Together, these studies support a role for NHERF-1 and NHERF-2 in regulating the distribution of Group II mGluRs in the murine brain, while conversely

Address for Correspondence: Randy A. Hall, Rollins Research Center, room 5113, 1510 Clifton Rd., Emory University School of Medicine, Atlanta, GA, USA, 30322, Phone: 404-727-3699, Fax: 404-727-0365, rhall3@emory.edu.

the effects of the mGluR2/3 PDZ-binding motifs on receptor signaling are likely mediated by interactions with other PDZ scaffold proteins beyond the NHERF proteins.

Keywords

astrocyte; NHERF; protein-protein interaction; knockout mice; electron microscopy; pre-synaptic; axon

Introduction

Metabotropic glutamate receptors are important regulators of glutamatergic and non-glutamatergic neurotransmission. This family of 8 G protein-coupled receptors is typically divided into three sub-families, Group I (mGluR1 & mGluR5), Group II (mGluR2 & mGluR3) and Group III (mGluR4, mGluR6, mGluR7 & mGluR8) on the basis of sequence homology. The members of the mGluR family are intriguing therapeutic targets for the treatment of various neurodegenerative and neuropsychiatric disorders. In particular, Group II mGluRs are potential targets for the treatment of schizophrenia, depression, Parkinson's Disease and drug addiction, with several mGluR2/3-targeted ligands advancing into clinical trials in the past few years (Vinson and Conn, 2012, Nicoletti et al., 2015).

G protein-coupled receptor signaling and trafficking can often be strongly influenced by receptor-interacting proteins (Ritter and Hall, 2009). Thus, the identification of the set of proteins capable of regulating Group II mGluRs may shed light on cell-specific regulation of these receptors and moreover present potential new therapeutic opportunities beyond the development of orthosteric and allosteric receptor-targeted ligands. A handful of Group II mGluR-interacting partners have been identified thus far, including tamalin (Kitano et al., 2002), protein kinase A or PKA (Schaffhauser et al., 2000, Cai et al., 2001), G protein receptor kinases or GRKs (Iacovelli et al., 2009), beta-arrestins (Iacovelli et al., 2009), RanBPM (Seebahn et al., 2008), PICK1 (Hirbec et al., 2002), GRIP (Hirbec et al., 2002) and protein phosphatase 2C or PP2C (Flajolet et al., 2003). Both mGluR2 and mGluR3 contain a motif on their C-termini that conforms to a consensus motif for interaction with PDZ domains, which are modular protein-protein interaction domains of approximately 90 amino acids in length (Sheng and Sala, 2001). Indeed, three of the aforementioned binding partners, tamalin, PICK1 and GRIP, have been shown to associate with mGluR2/3 via their PDZ domains (Kitano et al., 2002; Hirbec et al., 2002). Given that there might be other PDZ proteins capable of modulating mGluR2/3 function, we utilized a proteomic array of 96 distinct PDZ proteins to screen for novel Group II mGluR-interacting partners that might modulate receptor function and/or localization and thereby shed new light on the regulation of Group II mGluR function.

Experimental Procedures

Overlay of PDZ Array

Fusion proteins were purified and overlays of the PDZ domain array were performed as previously described (Fam et al., 2005, He et al., 2006). Briefly, 1 μg of His- and S-tagged

PDZ domain fusion proteins were spotted onto nitrocellulose, dried overnight, and then overlaid with GST-alone (control), GST-mGluR2-CT, or GST-mGluR3-CT. Membranes were washed and incubated with an HRP-coupled anti-GST monoclonal antibody (Amersham Pharmacia Biotech) and binding of mGluR2-CT or mGluR3-CT fusion protein was visualized using enhanced chemiluminescence.

Cell Culture

HEK293T and astrocyte cultures were maintained in Glutamax™ DMEM (Invitrogen) containing 5% dialyzed FBS and 1% pen/strep in a humidified incubator at 37°C with 95% air and 5% CO_2 to regulate pH. Cortical secondary astrocyte cultures were prepared from neonatal mice (P0–P2) in the method of McCarthy and Vellis (McCarthy and de Vellis, 1980) with minor modifications. The day after plating astrocytes, cultures were vigorously shaken to dislodge contaminating cell types and media was replaced. Every three to four days media was changed and flasks would be manually shaken each time astrocytes were passaged. After primary cultures reached confluence, cultures were passaged using trypsin and grown to confluence again, where they were then split into wells for signaling studies. These “tertiary” astrocytes were typically used after 25–30 days in culture for experiments.

Transfection

Mock pcDNA3.1+ (Invitrogen), rat mGluR2 or mGluR3 (originally in pBK-CMV and provided by Jeff Conn, Vanderbilt University; subcloned into pcDNA3.1), human FLAG-NHERF-1 (pBK-CMV) and rabbit FLAG-NHERF-2 (pBK-CMV) cDNAs were verified by sequencing. For HEK293T studies, Lipofectamine 2000 was used for transient transfections in accordance with manufacturer’s instructions. Endotoxin-free cDNAs were used with TransIT®-LT1 (Mirus) transfection reagent for all astrocyte experiments in accordance with the manufacturer’s instructions. In brief, a total of 2.5 μg of cDNAs were transfected per well of a 6-well plate. DNA complexes were mixed with opti-MEM supplemented with Glutamax™ and the TransIT®-LT1 reagent at a 3:1 ratio for 20 minutes prior to drop-wise addition to confluent astrocyte cultures. Experiments were performed 24–48 hours after transient transfection.

Site-Directed Mutagenesis

Mutagenesis of the last amino acid of the mGluR2 or mGluR3 was accomplished in accordance with the manufacturer’s instructions, using Quikchange Site-directed mutagenesis (Stratagene). Primers used for mGluR2 L872A were forward 5′ GAC TCA ACA ACG TCG TCG GCT TGA AGA TCC CAC ACT CC 3′ and reverse 5′ GGA GTG TGG GAT CTT CAA GCC GAC GAC GTT GTT GAG TC 3′. Primers used for mGluR3 L879A were forward 5′ GAC TCC ACC ACC TCA TCT GCG TGA CTC GA 3′ and reverse 5′ CCT CGA GTC ACG CAG ATG AGG TGG TGG A 3′. Primers were purchased from integrated DNA technologies (IDT) and were PAGE purified. All constructs were verified using sequencing.

Immunoprecipitation

Following transient transfection, cells were washed twice with ice-cold PBS supplemented with calcium to remove albumin. Cells were lysed with 1 ml of ice-cold harvest buffer (10 mM HEPES, 50 mM NaCl, 5 mM EDTA, 1% triton-X-100, and 1 protease inhibitor cocktail tablet (cOmplete, EDTA-free, Roche)). Membrane proteins were solubilized at 4°C with end-over-end rotation for one hour and subsequently centrifuged at 13,000 RPM to pellet insoluble fraction. A sample of the soluble lysate was saved and diluted with 6X Laemmli buffer to a 1X concentration, while remaining soluble lysate incubated with FLAG-agarose (Sigma) for one to two hours to immunoprecipitate FLAG-tagged NHERF proteins. Immunoprecipitate samples were sequentially washed three times with ice-cold harvest buffer and gentle vortexing and then eluted with 2X Laemmli buffer and left to denature for 18 to 24 hours prior to use. Samples from soluble lysates and immunoprecipitates were subjected to SDS-PAGE and Western analysis.

Astrocyte Signaling Studies

Six-well plates of tertiary astrocyte cultures were transiently transfected with endotoxin-free cDNAs encoding pcDNA3.1+, mGluR2, or mGluR3 as described above. After 24 hours, cells were washed three times and serum starved in 1 ml of incomplete Glutamax™ DMEM for 3–5 hours prior to stimulation with media (vehicle) or 1 μM LY354740 (Tocris) dissolved in 100 mM NaOH to neutralize the acid and diluted in incomplete media to a final 2X concentration. Application of 1ml of this 2X drug was applied to duplicate wells of cells that had been starved in 1 ml of media, so that the drug was a final 1X concentration. This method of drug application was found to not induce erroneous increases in phospho-ERK activation, which were observed just by the aspiration and replacement of media (vehicle) within a well. After treatment, media was rapidly aspirated and cells were lysed in 2X Laemmli buffer. Samples were then sonicated and stored at −20°C if not needed.

SDS-PAGE and Western Blot Analysis

Prior to use, any frozen samples were thawed and vortexed to dissolve precipitated SDS. Proteins were then subjected to SDS-PAGE using 4–20% tris-glycine gels. Proteins were then transferred onto nitrocellulose. For AKT signaling studies, membranes were blocked using Odyssey blocking buffer (LI-COR) and two fluorescent secondaries were used for simultaneous probing of phospho- and total AKT proteins. Primary antibodies used for AKT and ERK signaling studies were: rabbit monoclonal anti-phospho AKT (Ser473) XP clone D9E, (Cell Signaling Technology, catalog # 4060), rabbit monoclonal anti-phospho AKT (Thr308), clone C31E5E, (Cell Signaling Technology, catalog # 2965), mouse monoclonal total anti-AKT (pan), clone 40D4, (Cell Signaling Technology, catalog # 2920), rabbit monoclonal total anti-ERK 1/2, (Cell Signaling Technology, catalog # 9102), and mouse monoclonal anti-phospho ERK, clone E-4, (Santa Cruz Biotechnology, catalog # sc-7383). Primaries used for immunoprecipitation and/or expression studies were: rabbit polyclonal anti-mGluR2/3 (Chemicon, catalog # 06-676), mouse monoclonal anti-mGluR3 (MAb Technologies, catalog# GRM3-2), rabbit polyclonal anti-NHERF-1 (Ab 5199) from (Yun et al., 2002) or rabbit polyclonal anti-NHERF-2 (Ab 2570) from (Yun et al., 1998), and rabbit monoclonal anti-actin (Sigma, catalog # A2066). Following incubation in primary antibody

(overnight for signaling antibodies and 1 hr at room temperature for other antibodies), membranes were washed for 3 × 5 minutes and then incubated with the corresponding fluorescent secondary for signaling experiments (anti-mouse or anti-rabbit Alexa Fluor 680, Sigma, and anti-mouse or anti-rabbit IR-dye 800CS, LI-COR) or with the corresponding HRP-conjugated secondary (GE Healthcare, ECL™ anti-mouse or rabbit IgG, HRP-linked, whole antibody) for 30 minutes. The membrane was then washed 3 × 10 minutes and rinsed once with deionized water. Fluorescent bands were visualized using the Odyssey Imaging System (LI-COR) and quantified using Image Studio 1.1, according to the manufacturer's instructions. Chemiluminescent bands were visualized using an enhanced chemiluminescence kit (Pierce) and exposed to films for various time-points. The membrane was then stripped with Restore Buffer (Pierce) and probed with rabbit anti-actin (Sigma) as an internal control for protein loading.

C57BL6J (wild-type), NHERF-1 KO, and NHERF-2 KO mice

All mice were treated in accordance with IACUC guidelines at Emory University. Both NHERF-1 KO and NHERF-2 KO mice are congenic on C57BL6J (JAX). Thus, wild-type mice (hereafter referred to as WT mice) were littermate controls from either NHERF-1 KO or NHERF-2 KO mice. NHERF-1 KO mice (hereafter referred to as N1 KO mice) were originally created by Ed Weinman (University of Maryland) via a neomycin insertion into exon 1 (Shenolikar et al., 2002), while NHERF-2 KO mice (hereafter referred to as N2 KO mice) were originally created by Lexicon Genetics via a lentiviral gene trapping cassette (clone OST2298) found to be inserted into the intronic region after exon 2 (Singh et al., 2009) and provided by the lab of C. Chris Yun (Emory University). Primers were used to genotype mice and set-up breeders.

Genotyping

In accordance with IACUC guidelines, tail clips were taken from mice at P11 to P14 postnatal. Tails were then digested with a protease buffer (Proteinase K 2 mg/ml, SDS, EDTA, NaCl) overnight at 55°C and subsequently mixed with isopropranol to precipitate DNA. Approximately 500 ng of DNA were used for each PCR cycle. Primers for NHERF-1 were originally developed by (Shenolikar et al., 2002). They are P1 (Common Forward): 5′ CTC TGT TTA TTC CCA GAA GGA 3′; P2 (Neomycin Cassette, Mutant): 5′ CAA GAA GGC GAT AGA AGG CGA TG 3′; and P3 (WT Reverse): 5′ GAG CCA GGT TCT ACC AGA CGG ATA AAC TGG 3.′ PCR results were run on a 0.8% agarose gel with ethidium bromide to reveal PCR products. Primer combinations of P1 and P2 yielded a 2400 bp fragment that corresponded with the NHERF-1 mutant allele, while primer combinations of P1 and P3 yielded a 1400 bp fragment that corresponded with the WT NHERF-1 allele. The primers for NHERF-2 were originally developed by the Yun lab (Singh et al., 2009). They are P1 (Common Forward): 5′ TTC TAT AAG CCT CCA TTT CCT CT 3′; P2 (WT Reverse): 5′ CCC ACC CCC ATC GCT GCT C 3′; and P3 (Mutant Reverse): 5′ GCG CCA GTC CTC CGA TTG A 3′. PCR results were run on a 2.0% agarose gel with ethidium bromide to reveal PCR products. Primer combinations of P1 and P2 yielded a 303 bp fragment corresponding with the NHERF-2 mutant allele, while primer combinations of P1 and P3 yielded a 229 bp fragment corresponding to the WT NHERF-2 allele. Negative

control reactions in which the DNA was not included were also run to control for contamination.

siRNA Knockdown

Control siRNAs (Silencer Negative Control #1) and NHERF-1 silencer select siRNAs were purchased from Ambion®, ThermoFisher Scientific (catalog # 4390771, targets mouse exon 1). siRNAs stocks were reconstituted at 100 μM and dissolved in PCR-grade water, and stored at −80°C, until needed. In accordance with the manufacturer's instructions, cultured astrocytes were nucleofected with either control or NHERF-1 siRNA, using the AMAXA Basic Mammalian Glial Cells kit (Lonza). Following 72 hours of expression, astrocytes were lysed and examined for NHERF-1 and NHERF-2 levels. Signaling studies were also performed at the 72 hour time point.

Euthanasia and Tissue Collection

All mice used in the study were euthanized in accordance with IACUC guidelines. Adult mice were used for the expression studies across WT, N1 KO, or N2 KO genotypes and were euthanized via CO_2 asphyxiation. Following absence of toe pinch reflex, mice were rapidly decapitated and brains were quickly removed. Samples from prefrontal cortex, striatum, hippocampus and cerebellum were micro-dissected and immediately flash frozen on dry ice and stored at −80°C until needed.

Preparation of Brain Homogenates and Normalization of Protein Concentrations

To create the brain homogenates, snap frozen WT, N1 KO and N2 KO brain samples were thawed sequentially on ice in 10 ml of ice-cold harvest buffer containing 50 mM NaCl, 20 mM Hepes, 5 mM EDTA, 1 protease inhibitor cocktail tablet (Roche Applied Science, cat. # 04693132001), diluted with dH_2O up to 50 ml, pH 7.4. After thawing, the brain samples were subjected to 15 strokes in a dounce homogenizer to homogenize tissue and lyse cells. The crude homogenates were centrifuged for 15 minutes at 17,000 RPM (~35,000 g) at 4°C. The supernatants were discarded and the pellets were re-suspended in ice-cold harvest buffer, snap frozen in liquid nitrogen, and stored at −80°C until needed. Brain homogenates were thawed on ice and protein assays were performed (B.C.A. Pierce) to determine the protein concentrations of the samples. Samples were then re-suspended in 6× sample buffer to achieve a 1× final concentration.

Perfusions

A total of 12 mice were perfused for the electron microscopy experiments. Mice were acclimated for 2 hours prior to being deeply anesthetized with an overdose of ketamine (120 mg/kg, ip) and xylazine (16 mg/kg, ip). After checking for the absence of a toe-pinch reaction, mice were then transcardially perfused with ice-cold Ringer's solution, followed by a fixative containing 4% paraformaldehyde and 0.1% glutaraldehyde in phosphate buffer (0.1 M; pH 7.4, freshly prepared) at a slow, steady rate. After perfusion, mice brains were carefully removed from the skull and immediately transferred to a 4% paraformaldehyde solution to post-fix overnight. Additionally, a sample of tail was taken to confirm

genotyping. Brains were then serially sectioned into 60-μm-thick sections using a vibrating microtome and stored in phosphate-buffered saline (PBS) at 4°C until needed.

Primary Antibodies and Controls for Immunoelectron Microscopy

The primary antibody used (Millipore/Chemicon-AB1553, lot LV1825814) was raised against the C-terminal epitope (NGREVVDSTTSSL) that is highly similar to both mGluR2 and mGluR3. This antibody is highly specific has been used successfully by others to detect Group II mGluRs in the rodent brain; however, it does not distinguish between mGluR2 and mGluR3 (Petralia et al., 1996, Muly et al., 2007). In the present study, it was used at a dilution of 1:100 or 1.0 μg/ml.

LM Immunoreaction

Tissue sections were chosen from the same region of the cortex across all genotypes, as assessed via their location in the serial sectioning. Sections were then placed in a 1% sodium borohydride solution for 20 minutes and washed extensively with PBS (phosphate-buffered saline; 0.01M, pH 7.4) until bubbles had completely dissipated. Sections were incubated in blocking serum (1% normal goat serum, 1% bovine serum albumin, 0.3% Triton-X-100, diluted in PBS) for one hour at room temperature and were then incubated with the primary antibody (Ab 1553 anti-mGluR2/3 1:100 dilution in blocking serum) overnight at room temperature. Following removal of the primary antibody solution, sections were rinsed three times with PBS and then incubated with a 1:200 dilution of a biotinylated goat anti-rabbit IgG (Vector Laboratories, Burlingame, CA, USA) for one hour at room temperature. The sections were then rinsed three times with PBS and incubated for an additional 90 minutes in the avidin-biotin peroxidase complex (ABC) solution. Sections were then rinsed two times in PBS and then one final time in Tris-HCl buffer (0.05M, pH 7.6). Immediately prior to use, fresh 3,3′-diaminobenzidine (DAB) solution was prepared (using H_2O_2 and Tris-HCl) and then added to the sections to incubate for ten minutes to reveal the labeling. Sections were thoroughly rinsed at least five times and then carefully mounted onto gelatin-coated slides. The next day, they were cover-slipped for imaging and long-term storage. As controls, the reaction was performed as described, except the primary antibody was pre-adsorbed with ten times the relative amount of the mGluR2-CT peptide (Peptide 2.0, Chantilly, VA, USA) overnight at 4°C and then added to sections in order to measure background labeling. No significant labeling was detected, in accordance with previous reports regarding the specificity of this antibody (Petralia et al., 1996, Muly et al., 2007, Lavialle et al., 2011).

EM Reaction

Tissue sections were chosen from the same cortical region across all genotypes, as assessed via their location in the serial sectioning. Sections were washed 2× in PBS and then incubated in 1% sodium borohydride. Following extensive washing in PBS, sections were sequentially cryoprotected. Preembedding immunoperoxidase labeling was then performed. Sections were incubated in blocking solution (same as in the LM reaction, but excluding Triton-X-100) and then incubated in the primary antibody (Ab 1553 anti-mGluR2/3 1:100) for 36 hours at 4°C with gentle shaking. After the incubation, sections were rinsed three times in PBS and then incubated with a 1:200 dilution of a biotinylated goat anti-rabbit IgG (Vector Laboratories, Burlingame, CA, USA) for one hour at room temperature. The

sections were then rinsed three times with PBS and then incubated for an additional 90 minutes in the avidin-biotin peroxidase complex (ABC) solution. Sections were then rinsed two times in PBS and then one final time in Tris-HCl. Immediately prior to use, fresh 3,3′-diaminobenzidine (DAB) solution was prepared (using H_2O_2 and Tris-HCl) and then added to the sections to incubate for ten minutes to reveal the labeling. Sections were thoroughly rinsed at least five times and then carefully mounted onto gel-coated slides. Sections were then processed for electron microscopy by transferring to phosphate buffer (PB, pH 7.4) for 3 × 5 minutes washes and then subsequent treatment with 1% osmium tetroxide in PB to further fix and stain the tissue (20 minute incubation). Tissue was then sequentially dehydrated, beginning with incubation in 50% ethanol and then switching to 70% ethanol (supplemented with 1% uranyl acetate, filtered) for a 35-minute incubation in the dark, followed by incubations in 90% and 100% ethanol solutions. Sections were then treated with propylene oxide and immersed in freshly prepared Durcupan resin, mounted onto slides, coverslipped and baked overnight to harden. Small samples of tissue were then chosen from similar regions of the frontal cortex across all groups and mounted onto resin blocks to be processed for ultra-thin sectioning. Ultra-thin sections (60 nm) were collected and mounted onto Pioloform-coated copper grids. All grids were counterstained with lead citrate for 5 minutes prior to imaging.

Image Acquisition and Analysis

For the analysis of the relative distribution of Group II mGluRs labeling across elements and for the determination of the density of labeling, approximately 50 micrographs were randomly taken of any labeled elements at 40 000X. Generally, images were acquired approximately one-two fields of view from the resin-tissue interface allowing for sufficient antibody penetration and ultrastructural integrity. From each of these images, a scorer, blinded to the animal genotype, identified and counted the different mGluR2/3-immunoreactive elements in the tissue based on ultrastructural criteria established by Peters et al (Peters et al., 1991). Given the significant glial labeling observed as well as the fact that much of this labeling appeared to associate with asymmetric synapses and thereby correspond to perisynaptic astrocyte processes (PAPs), glial Group II mGluR labeling was further sub-divided into perisynaptic or non-perisynaptic astrocyte processes. Astrocyte processes are known to be intimately associated with synapses, but variations in the extent of astrocyte coverage, as assessed in two-dimensional micrographs, are often observed. Consequently, PAPs were defined into three categories, based on their extent of association with pre- and post-synaptic elements and their distance from the post-synaptic density specializations. PAP-A astrocytes had labeled processes that were in contact with both the pre- and the post-synaptic neuron; PAP-B astrocytes had labeled processes that were touching either the pre- or the post-synaptic neuron; and PAP-C astrocytes corresponded to astrocytes with labeled processes distal from the synapse. From these data, the average relative densities (+/− SEM) of labeled elements were calculated and statistically compared between animal groups.

Results

Screening of a PDZ proteomic array for Group II mGluR-interacting partners

A proteomic array of 96 distinct PDZ domains was screened with GST fusion proteins comprising the last 25 amino acids of the C-termini (CT) of mGluR2 or mGluR3. The two GST fusion proteins bound to a small set of PDZ proteins, while matching control overlays with GST alone resulted in little to no background binding (Figure 1). The mGluR2-CT (Figure 1A) and mGluR3-CT (Figure 1B) bound robustly to PDZ domains from the Na+/H+ Exchanger Regulatory Factors 1 and 2 (NHERF-1 and -2). In particular, mGluR2-CT robustly bound to PDZ domains 1 and 2 of both NHERF-1 and NHERF-2, while mGluR3-CT bound robustly to both PDZ domains of NHERF-2 and the first PDZ domain of NHERF-1, yet bound only weakly to the second PDZ domain of NHERF-1. Of noteworthy interest, mGluR3-CT, as well as to a lesser extent mGluR2-CT, also bound to the cystic fibrosis transmembrane conductance regulator-associated ligand (CAL; also known as PIST, GOPC, and FIG). Importantly, only a handful of additional weak interactions were detected (Figure 1C), increasing confidence in the specificity of the observed associations.

Both NHERF-1 and NHERF-2 contain two tandem PDZ domains and a C-terminal ezrin-radixin-moesin (ERM)-binding domain that can tether the scaffolds to the actin cytoskeleton via ERM protein association. A number of previous studies have demonstrated regulation of G protein-coupled receptors by the NHERF proteins (Ardura and Friedman, 2011). More pertinently, NHERF-2 has been shown to be an interacting partner for the metabotropic glutamate receptor mGluR5 (Paquet et al., 2006a), and both NHERF-1 and NHERF-2 have also been shown to associate with the astrocytic glutamate transporter GLAST (Ritter et al. 2011). Therefore, we endeavored to explore how interaction with NHERF-1 and/or NHERF-2 might regulate Group II mGluR function.

Validation of the NHERF proteins as interacting partners for Group II mGluRs

As initial identification of the Group II mGluR and NHERF interaction relied solely on the receptors' C-termini, we next assessed whether full-length mGluR2 and mGluR3 might associate with the NHERF proteins in a cellular context. To this end, co-immunoprecipitation experiments were performed using human embryonic kidney (HEK293T) cells that were transiently transfected with cDNAs encoding pcDNA3.1 (mock vector), rat mGluR2, rat mGluR3, FLAG-tagged NHERF-1 and/or FLAG-tagged NHERF-2. Immunoprecipitation of FLAG-tagged NHERF-1 or NHERF-2 resulted in the robust co-precipitation of both mGluR2 (Figure 2A) and mGluR3 (Figure 2B). Interestingly, a higher fraction of cellular mGluR3 consistently associated with both NHERF-1 and NHERF-2, relative to mGluR2, highlighting a potential difference between these two receptors and their ability to interact with the NHERF proteins. It should be noted that HEK-293T cells express endogenous NHERF-1 and -2, as seen in the lysates in Fig. 2, but these endogenous NHERF proteins did not impact the co-immunoprecipitation, which was directed at the FLAG epitope of the transfected proteins.

Interaction of type 1 PDZ proteins with their cellular partners is usually, but not always, dependent on the last few amino acids of the interacting partners (Doyle et al., 1996,

Niethammer et al., 1998). To this end, the last amino acid of both the mGluR2 and the mGluR3 CT was mutated from a leucine to an alanine (L872A and L879A respectively). It was then examined if these mutant constructs could associate with the NHERF proteins via co-immunoprecipitation. Both mGluR2 L872A (Figure 2A) and mGluR3 L879A (Figure 2B) bound poorly to either NHERF protein, demonstrating the requirement of this last amino acid for NHERF interaction and the creation of useful tools for studying how direct interaction with PDZ ligands might regulate mGluR function.

Identification of cultured astrocytes as a model system to study NHERF regulation of Group II mGluR signaling

After establishing that full-length NHERF proteins can associate with Group II mGluRs, we set out to determine how these interactions might regulate receptor function. However, initial studies in which we endeavored to measure mGluR3 signaling in HEK-293T cells failed to elicit a robust and reliable mGluR3-dependent signaling. In fact, challenges in studying mGluR3 signaling in heterologous over-expression systems have been frequently reported (Schoepp et al., 1997, Wroblewska et al., 1997, Wroblewska et al., 2011, Diraddo et al., 2014), corroborating our inability to measure a robust mGluR-dependent functional signal in HEK293T cells. In order to circumvent these issues, we decided to employ cultured astrocytes as a model system to compare mGluR2 and mGluR3 signaling and study how both receptors might be regulated by the NHERF proteins. Cultured astrocytes are known to express both NHERF-1 and NHERF-2 and also express high levels of endogenous GLAST (Ritter et al., 2011). Interestingly, Schoepp and colleagues have previously had marked success with measuring mGluR signaling in heterologous expression systems in which GLAST was also overexpressed, presumably due to GLAST-mediated decreases in extracellular glutamate concentrations (Schoepp et al., 1997). Thus, cultured astrocytes would be expected to recapitulate this scenario. Moreover, cultured astrocytes have been reported to express endogenous mGluR3, and activation of astrocytic mGluR3 has been shown to signal to such intracellular effectors as extracellular regulated kinase (ERK), AKT (also known as protein kinase B or PKB), and adenylyl cyclase (Bruno et al., 1997, Bruno et al., 1998, D'Onofrio et al., 2001, Moldrich et al., 2002, Aronica et al., 2003, Ciccarelli et al., 2007, Durand et al., 2010). However, despite employing a variety of astrocyte culturing methods, we were unable to detect expression of endogenous astrocytic mGluR3 protein via Western blot and also did not observe any functional evidence that mGluR3 was endogenously present in our astrocyte cultures. Thus, our conclusion was that Group II mGluR expression was lost during the culturing process of our astrocyte cultures.

Given the lack of endogenous Group II mGluR expression in our primary astrocyte cultures, we decided to reintroduce Group II mGluRs back into these astrocyte cultures via transfection. Since we wanted to compare NHERF regulation of both mGluR2 and mGluR3, we also performed studies in which we separately expressed either mGluR2 or mGluR3. As mentioned above, there is extensive evidence that mGluR3 is widely expressed in astrocytes in many brain regions *in vivo* (Ohishi et al., 1994, Petralia et al., 1996, Tamaru et al., 2001, Muly et al., 2007, Sun et al., 2013), and expression of mGluR2 has been described in certain populations of astrocytes as well (Phillips et al., 2000). Of the two primary signaling effectors examined, ERK and AKT, we observed the most robust increases in mGluR-

mediated AKT signaling. Thus, subsequent studies compared the abilities of mutant mGluR2 L872A and mGluR3 L879A to signal to AKT, as NHERF proteins have been shown to negatively regulate AKT signaling that is downstream of receptor tyrosine kinases (Takahashi et al., 2006, Pan et al., 2008).

Group II mGluR-mediated AKT signaling in cultured astrocytes is regulated by the PDZ-interacting motif

Examination of mGluR2 versus mGluR2 L872A signaling in the primary astrocytes revealed that mutant mGluR2 signaled more robustly to AKT, as assessed by increased ratios of phosphorylated Ser473 normalized to total AKT (Figure 3A–B, Two Factor ANOVA, $p < 0.05$, receptor). This difference did not reflect a difference in the time course of AKT signaling, as there was no difference in the magnitude of the effect at different time points (Two Factor ANOVA, $p > 0.05$, time). In contrast, mGluR3 and mutant L879A signaled to AKT comparably, both with a much smaller fold increase in AKT phosphorylation than was observed for mGluR2 (Figure 3C–D). These data provide evidence that disruption of PDZ domain interactions with the C-terminus of mGluR2 can negatively regulate downstream mGluR2-mediated AKT signaling.

In order to determine if interactions with the NHERF proteins, as opposed to other PDZ partners, were important for modulation of mGluR2 signaling to AKT, we endeavored to examine mGluR2 and mGluR3 signaling in astrocytes in which endogenous NHERF-1 and NHERF-2 were not expressed. To address this question, we first confirmed that each respective NHERF protein was absent in the brain from NHERF-1 (N1) KO or NHERF-2 (N2) KO mice by examining NHERF-1 and NHERF-2 expression levels in various brain regions using polyclonal antibodies that have been extensively characterized, (Lamprecht et al., 1998, Yun et al., 1998). Indeed, full-length NHERF-1 was not detected in brain lysates from N1 KO mice (Figure 4A). Full-length NHERF-2 was also not detected in brain lysates from N2 KO mice (Figure 4B) in agreement with previous reports (Broere et al., 2007), although we cannot exclude the possibility that the unknown band evident in Figure 4B might correspond to a small amount of residual NHERF-2 protein with an abnormal molecular weight. Additionally, total levels of the full-length NHERFs did not change in the respective NHERF KO mouse brain samples, suggesting there was not a compensatory up-regulation of one NHERF protein when the other was knocked out. Interestingly, the NHERF-2 antibody detected a distinct band in the N2 KO brain tissue samples. This band migrated on SDS-PAGE gels at approximately 27 kDa and exhibited a distinctive pattern of expression across the three genotypes studied: it was significantly increased in all three N2 KO mouse brain samples and slightly decreased in all three N1 KO mouse brain samples, relative to wild-type (WT) samples. We hypothesized that this band may be a splice variant of NHERF-2 and indeed a NHERF-2 splice variant has been reported to exist in peripheral tissue (Fouassier et al., 2001). Further, Genbank searches revealed reports of a NHERF-2 transcript variant that is present in both mouse and humans and encodes a truncated version of NHERF-2 that lacks the second PDZ domain and is predicted to be 24.5 kDa in mass. Analyses of the NHERF-2 full length mRNA and the NHERF-2 splice variant revealed them to differ in the intronic region in which the NHERF-2 retroviral gene-trapping cassette was initially inserted (Lexicon Genetics). Thus, the NHERF-2 splice variant would not have been

targeted by the gene trapping method, which supports the idea that the observed 27 kDa band that is upregulated in the NHERF-2 KO brain tissue is indeed the protein product of the shorter NHERF-2 transcript variant.

We then compared mGluR-mediated AKT responses in astrocyte cultures prepared from WT, N1 KO, and N2 KO astrocytes. As we were unable to successfully generate double N1/2 KO mice on the C57BL6/J background (see section below on hydrocephaly), N2 KO astrocytes were treated with control siRNA or NHERF-1 siRNAs to create a NHERF-1/-2 null state. However, no differences were observed when comparing mock, mGluR2, or mGluR3 responses across all culture types for Ser473-mediated AKT responses (Figure 4C). Additionally, it was confirmed that substantial knockdown of NHERF-1 was achieved (Figure 4D) in the N2 KO cultures, thereby creating a condition in which little full length NHERF proteins would be expressed. These data suggest that loss of NHERF-1, NHERF-2, or both NHERF proteins does not affect Group II mGluR-mediated AKT responses in cultured astrocytes.

A potential role for the NHERFs in Group II mGluR cellular and subcellular localization

Given that the signaling studies revealed an important role for the PDZ-binding motif, but not the NHERF proteins, in regulating Group II mGluR signaling to AKT, we next examined potential effects of the NHERF proteins in regulating the localization of Group II mGluRs. It has been shown that Group II mGluRs and mGluR5 (Hubert and Smith, 2004, Sun et al., 2013) are detected in glial processes that ensheath asymmetric synapses in the hippocampus of rodent brain, a particular compartment of astrocytes termed the perisynaptic astrocyte process, or PAP (Lavialle et al., 2011). Additionally, ezrin, an actin-binding protein, has also been shown to be particularly abundant in this perisynaptic compartment and does not appear to overlap with the intermediate filament protein GFAP (Derouiche and Frotscher, 2001, Derouiche et al., 2002, Lavialle et al., 2011). Analysis of the relative distribution of NHERF-2 in the rodent brain revealed it is most commonly found in glia. Although examples of NHERF-2 labeling in the PAP have been reported, these data have not been quantified (Paquet et al., 2006b). Given the presence of the ezrin-radixin-moesin (ERM) binding domain on both NHERFs, we hypothesized that the NHERF proteins might be critical regulators of Group II mGluR trafficking *in vivo*, potentially influencing mGluR overall expression levels and/or targeting the mGluRs to ezrin-enriched PAPs.

As a first step, we examined if expression levels of Group II mGluRs might be altered in the NHERF KO brain tissue, and found that loss of either NHERF-1 or NHERF-2 did not change total expression levels of Group II mGluRs in the cortex, striatum, hippocampus, or cerebellum, as compared to brain homogenates from WT age- and sex-matched mice (analysis of variance by One-Way ANOVA: cortex, $p = 0.47$; striatum, $p = 0.11$; hippocampus, $p = 0.12$; cerebellum, $p = 0.11$; $n = 3$ per group, data not shown). Then, we used immuno-electron microscopy (EM) to assess potential changes in the ultrastructural localization of Group II mGluRs in brain tissue in N1 and/or N2 KO mice.

Ultrastructural localization of Group II mGluR labeling in the cerebral cortex of N1 KO and N2 KO mice

Single immunoperoxidase labeling for Group II mGluRs was performed across WT, N1 KO, and N2 KO mice. Neuronal and glial elements were classified based on ultrastructural criteria established by Peters et al. (Peters et al., 1991). Representative images of Group II mGluR labeling across WT (Figure 5A), N1 KO (Figure 5B), and N2 KO (Figure 5C) mice are shown in Figure 5. Quantification of these images across genotypes revealed that Group II mGluR labeling was primarily observed in glia and unmyelinated pre-terminal axons, with labeling less commonly seen in axon terminals or post-synaptic structures such as dendrites and spines (Figure 5D). Interestingly, comparisons of the relative distribution of Group II mGluR labeling indicated that WT and N1 KO mice had a comparable distribution of Group II mGluR immunoreactivity, with approximately 55% of the labeling found in glial processes and 40% of the labeling associated with unmyelinated axons. In contrast, an increased axonal versus glial Group II mGluRs labeling was observed in N2 KO mice, relative to WT and N1 KO mice (Figure 5D). No appreciable differences in the overall density of labeled glia were observed across the various genotypes (Figure 5E), suggesting that the shift in the Group II mGluR distribution in the N2 KO mice was due to an increase in axonal Group II mGluR labeling and not a decrease in glial labeling. Additionally, quantification of the proportion of Group II mGluR-immunoreactive glial processes in the mouse cortex revealed that 47.5% ± 1.24% (mean ± S.E.M.) of all perisynaptic glial processes are labeled for Group II mGluRs, implying a significant function for Group II mGluRs in peri-synaptic glia which, based on morphological criteria, most likely correspond to astrocytes. Moreover, we also counted the number of asymmetric synapses across groups and found them to be statistically indistinguishable (One-way ANOVA, Tukey's multiple comparisons, n.s.), with mean synapse densities per 100 μm^2 ± S.E.M. being 32.0 ± 1.9, 38.0 ± 5.3, and 31.8 ± 1.6, corresponding to counted synapses in WT, N1 KO, and N2 KO mice respectively.

Given the significant glial labeling observed as well as the fact that much of this labeling appeared to associate with asymmetric synapses and thereby correspond to perisynaptic astrocyte processes (PAPs), the glial Group II mGluR labeling was further sub-divided into perisynaptic or non-perisynaptic astrocyte processes. Astrocyte processes are known to be intimately associated with synapses, but variations in the extent of astrocyte coverage, as assessed in two-dimensional micrographs, are often observed. Consequently, PAPs were defined into three categories based on their extent of association with pre- and post-synaptic elements and their distance from the post-synaptic density specializations (see Methods: Image Acquisition and Analysis, and Figure 6A–B). The relative distribution of Group II mGluR-labeled perisynaptic processes versus non-perisynaptic processes was examined across groups. Few meaningful differences were observed (Figure 6C) and an analysis of mean densities did not support any significant differences in any PAP or non-PAP distributions across genotypes (Figure 6D). Similar results were obtained when PAP categories were collapsed (Figure 6E–F).

Finally, comparisons of labeled and non-labeled PAP-A were made across genotypes, corresponding to the most stringent classification of the PAPs, ultimately revealing that there

were no significant differences in the mean densities of the proportion of Group II mGluR-labeled PAP-A versus non-labeled PAP-A across genotypes (Two-way ANOVA, genotype and labeling, n.s.). Although an analysis of the relative distribution of labeled versus non-labeled Group II mGluR PAP-A in WT mice revealed that 38.7% ± 2.0 (mean ± S.E.M.) of PAP-A in WT cortex are Group II mGluR-immunopositive, while 50.5% ± 2.9 or 48.5% ± 1.5 of total counted PAP-A are Group II mGluR-immunopositive in N1 and N2 KO mice, respectively, these differences in relative distribution are challenging to interpret because the mean densities are not statistically different. In summary, approximately 39% of identified PAP-A in WT mice are immunolabeled for Group II mGluRs, highlighting the functional role of these receptors in this anatomical compartment.

Experimental observations suggest a role for NHERF proteins in hydrocephaly and implicate NHERFs in CNS function

Sections from N1 KO and N2 KO mice consistently had much larger ventricles, relative to their WT littermates (Figure 7A). This was observed for all 6 NHERF KO mice used in this immuno-electron microscopy study. These results are consistent with the hydrocephaly phenotype observed in the N1 KO mice, (Figure 7B) as during the course of our studies on NHERF-1 adult mice we observed about a more than 30% incidence of confirmed hydrocephaly in the colony. Hydrocephalic mice were identified based on the presence of key features such as an abnormal, enlarged head and appearance of swollen eyes; this assessment was also informed by conversations with veterinary staff. We also observed hydrocephaly in female mice, but as male mice were used for all studies, fewer female mice were kept and monitored and reliable quantitative estimates cannot be made.

Discussion

Group II metabotropic glutamate receptors, comprising mGluR2 and mGluR3, are of particular interest as modulatory CNS targets, with excitement focusing on targeting Group II mGluRs for the treatment of schizophrenia (Patil et al., 2007). More recently, targeting the proteins that interact with mGluRs has been identified as an additional strategy for regulating glutamatergic transmission (Enz, 2012). In this study, Group II mGluR C-termini were screened against a PDZ proteomic array and found to selectively associate with NHERF-1 and NHERF-2. These findings expand upon the components of the astrocytic glutamate signaling system that NHERFs are known to bind to and regulate, to include the glutamate transporter GLAST (Ritter et al., 2011) and another metabotropic glutamate receptor, mGluR5 (Paquet et al., 2006a). Both mGluR2 and mGluR3 were found to associate with NHERF-1 and NHERF-2 in cells, with a higher fraction of cellular mGluR3 (relative to mGluR2) being co-immunoprecipitated with the NHERF proteins. Mutation of the last amino acid of mGluR2 or mGluR3 was found to be sufficient to disrupt NHERF-1 and NHERF-2 association, thereby providing insight into the structural determinants of the interactions. Disruption of the C-terminal PDZ-interacting motif of mGluR2 was found to enhance receptor-mediated activation of AKT in astrocytes; however, this effect was probably not due to disruption of associations with the NHERF proteins, since the effects of the mutation were not recapitulated by knock-out or knockdown of NHERF-1 or NHERF-2.

Furthermore, we examined how the NHERF proteins might regulate Group II mGluRs *in vivo*. An electron microscopic examination of the cellular and sub-cellular distribution of Group II mGluRs in the mouse cortex in wild-type, N1 KO, and N2 KO mice, revealed that loss of NHERF-2 led to a modest redistribution in the cellular targeting of Group II mGluRs to pre-terminal unmyelinated axons, without altering overall Group II mGluR expression. These studies support a role for NHERF-2 in directing the cellular localization of Group II mGluRs in the murine cortex thereby enhancing our understanding of the molecular mechanisms underlying both normal regulation and potential dysregulation of glutamatergic neurotransmission. However, a number of conclusions regarding the study of Group II mGluR signaling, the physiological relevance of cultured astrocytes, and what role NHERF proteins might play in CNS function have also arisen that will be described in greater detail below.

Reconciliation of cultured versus *in vivo* astrocytes: A case study on mGluR3

Due to the fact that studying Group II mGluR signaling in HEK293T cells proved challenging, we studied Group II mGluR signaling in cultured astrocytes. However, one major complication in these signaling studies was the persistent need to transfect mGluR2/3 into our cultured astrocytes. Indeed, it may have been easier to discern the effects of knocking out the NHERF proteins if signaling by endogenous Group II mGluRs was being measured. Although the expression of mGluR3 in astrocytes has been well-documented using *in vivo* approaches, including both *in situ* hybridization (Tanabe et al., 1993, Testa et al., 1994) and immunohistochemical approaches (Ohishi et al., 1994, Petralia et al., 1996, Tamaru et al., 2001, Muly et al., 2007, Sun et al., 2013), the expression of Group II mGluRs in cultured astrocytes has been more controversial. In our studies, even when mGluR3 was re-introduced into the cultured astrocytes via transfection, only a small functional response to activating AKT was observed. Despite this concern, when these data are taken as a whole, it becomes apparent that mGluR3 expression was lost in our cultured astrocytes, which is in stark contrast to the significant fraction of glial Group II mGluR immunolabeling (presumably astrocytic) observed in the mouse cortex, in which approximately 47% of all identified glia were immunopositive.

Many groups who have explicitly examined mGluR3 protein expression in cultured astrocytes have reported difficulties with detecting mGluR3 protein via Western blot analysis (Bruno et al., 1997, Ciccarelli et al., 1997, Aronica et al., 2003). For example, Bruno and colleagues demonstrated that they could measure immunocytochemical reactivity of Group II mGluRs in mixed mouse neuron and astrocyte cultures, but when probing 60 μg of cell lysate from mouse or rat astrocyte cultures, no immunoreactivity was observed via Western blot analysis, despite positive detection of brain lysates (Bruno et al., 1997). They postulated that Group II mGluR expression levels (and presumably mGluR3) were too low in the cultures to be detected by Western blot (Bruno et al., 1997). Likewise, probing of 100 μg of cultured rat astrocyte lysate via Western blot analysis only resulted in the detection of mGluR5 and not mGluR3 (Ciccarelli et al., 1997). Ciccarelli and colleagues also commented that mGluR3 could not be detected in 150 μg of lysate, as measured using two different C-terminal mGluR2/3 antibodies and following immunoprecipitation of any mGluR2/3 that might have been present in their cultures (Ciccarelli et al., 1997). Similarly, Western blot

analysis of human astrocyte cell lysates has been shown to be sufficient to detect mGluR5 (30 μg protein sample), while mGluR3 (even 150 μg cell lysate sample) could not be readily detected (Aronica et al., 2003). However, it was more recently reported that Group II mGluRs can be detected under some conditions using Western blot analysis approaches in astrocyte cultures (Durand et al., 2010) and furthermore that treatment with lipopolysaccharide (LPS) can increase expression of mGluR3 (Durand et al., 2010). Moreover, the authors provided some immunocytochemistry of mGluR3 labeling in cultured astrocytes (Durand et al., 2010). In future work it will be of interest to determine why the expression of Group II mGluRs in cultured astrocytes can be so variable depending on culturing conditions. In any case, this discrepancy between the robust mGluR3 expression that is always observed in brain astrocytes and the often-undetectable mGluR3 levels in cultured astrocytes highlights a larger concern as to what extent cultured astrocytes recapitulate the properties of astrocytes from the brain.

This question has been extensively explored by other laboratories, in which comparisons were made of the transcriptome expression patterns of astrocytes acutely isolated from the developing rodent CNS versus primary astrocyte cultures grown in the presence/absence of serum (Cahoy et al., 2008). In line with the observations in our studies, of the 2000+ genes identified as being differentially expressed between isolated astrocytes and cultured astrocytes, comparison of the expression pattern of *Grm3* mRNA transcripts in cultured astrocytes prepared in the commonly used method of McCarthy and de Vellis (McCarthy and de Vellis, 1980) versus astrocytes isolated via FACS from various rodent post-natal days (P1, P7, or P17), revealed that expression for *Grm3* is more than 26-fold higher in acutely isolated astrocytes, relative to cultured astrocytes (see supplemental Table S20) (Cahoy et al., 2008). Moreover, when the Barres group applied a more sophisticated and demonstrably physiological immunopanning (IP) method to culturing astrocytes, versus the conventional McCarthy and de Vellis approach, IP-astrocytes that were cultured for 7 days *in vitro* (DIV) had a significant decrease (72 fold, $p < 0.05$) in *Grm3* transcripts, relative to IP-astrocytes from P1 brains (Foo et al., 2011). Comparisons of transcript expression of IP-astrocytes from P7 brains with IP-astrocytes from P7 brains that were subsequently cultured for 7 days *in vitro* also revealed that *Grm3* transcripts were decreased by 100 fold ($p < 0.05$) in the cultured astrocytes (Foo et al., 2011). Taken together, both studies from the Barres laboratory identify *Grm3* as a gene that is significantly downregulated during the astrocyte culturing process, even when an arguably more physiologically relevant method (Foo et al., 2011) is used to isolate astrocytes from rodent brains. Thus, it will be of future interest to determine how *Grm3* is being downregulated and under which conditions can astrocytes be cultured to express mGluR3.

A role for PDZ interactions in regulating mGluR2 signaling

Disrupting mGluR2 interactions with PDZ proteins in astrocytes resulted in enhanced receptor signaling to AKT. However, this effect was not recapitulated by deletion of NHERF proteins, which suggests that interactions with other PDZ partners are more salient for the observed effect on mGluR2 signaling. Possible candidates to mediate this effect include previously-identified PDZ partners of mGluR2/3 such as tamalin (Kitano et al., 2002), PICK1 (Hirbec et al., 2002), and GRIP (Hirbec et al., 2002), in addition to the candidate

Group II mGluR-interacting proteins identified in the PDZ array studies reported here. It should be pointed out that screening a larger portion of Group II mGluR C-termini than the portions screened here might facilitate the identification of additional candidate PDZ partners, since PDZ domains can recognize both C-terminal sequences and internal sequence motifs (Ivarsson, 2012). An additional limitation of the current study is that the co-immunoprecipitation experiments were performed using NHERF constructs from either human (NHERF-1) or rabbit (NHERF-2) in conjunction with rat Group II mGluRs. Given that the functional domains are highly conserved across species, with sequence identity conservation more than 85% across the different species used, the interactions described here are likely to be conserved across species. However, it cannot be ruled out that species differences could alter some of the interactions described.

It will furthermore be important for future studies to examine these additional PDZ-interacting partners to determine if loss of mGluR2 association with PDZ scaffolds distinct from NHERFs can regulate the magnitude of the mGluR2-mediated AKT signaling response. In summary, these data from the primary astrocyte studies reveal an important role for the PDZ-interacting motif on the mGluR2-CT in regulating receptor signaling to AKT, but it is unclear at present which PDZ binding partners are the relevant associations being disrupted.

A role for NHERF-2 in Group II mGluR neuronal localization in the brain

Our studies examining the relative distribution of Group II mGluR labeling expand on what is known about the cellular and subcellular distribution of mGluR2 and mGluR3 in the rodent brain. The anatomical findings are consistent with other reports demonstrating that Group II mGluR labeling can be observed in pre-terminal unmyelinated axons, glial processes, spines, dendrites, and axon terminals (Petralia et al., 1996, Tamaru et al., 2001, Muly et al., 2007, Sun et al., 2013). Based on mRNA studies in rodents, the Group II mGluR immunoreactivity observed in glia is thought to correspond with mGluR3 labeling of astrocytes and not mGluR2 (Tanabe et al., 1993, Fotuhi et al., 1994, Testa et al., 1994), although one report found otherwise (Phillips et al., 2000). More recently, the relative distribution of Group II mGluRs in the cortex and hippocampus was examined and found to also predominate in presynaptic elements and glia, with infrequent labeling observed in post-synaptic elements (Sun et al., 2013). However, Sun and colleagues reported enhanced Group II mGluR labeling in axonal elements, rather than glial elements, which may reflect differences in the area of cortex examined and/or the application of the criteria used to identify elements (Sun et al., 2013). Our studies build upon these findings by quantifying the proportion of Group II mGluR-immunoreactive elements in the cortex, as we found that Group II mGluR-immunoreactive glia in the WT animals corresponded to approximately 47% of all glia identified in the mouse cortex. This highlights a significant role of Group II mGluRs in glia, which based on morphological criteria, most likely correspond to astrocytes.

We also investigated the hypothesis as to whether loss of either NHERF protein would alter the glial localization of Group II mGluRs. Specifically, we hypothesized that fewer perisynaptic astrocyte processes, or PAPs, would be immunolabeled for Group II mGluRs in brain sections from NHERF KO mice. The rationale behind this hypothesis was that the

actin-binding protein ezrin has been shown to be enriched in PAPs (Derouiche and Frotscher, 2001, Derouiche et al., 2002) and NHERF-2, which contains an ezrin-radixin-moesin (ERM) binding domain, has also been found to be localized in PAPs (Paquet et al., 2006b). Surprisingly, no differences in mGluR2/3 PAP localization were observed across genotypes in our study, even when various PAP criteria were applied. Ideally, we would also have been able to explore a NHERF-1 and NHERF-2 double-KO state, as the possibility remains that expression of one NHERF protein might be able to functionally compensate for loss of the other NHERF protein. Moreover, technical challenges exist with identifying PAPs in two-dimensional images, as a high frequency of false negatives is possible, especially when using the most stringent PAP criteria to only score labeled glial processes that physically touch the pre- and post-synaptic elements of an asymmetric synapse. Future studies in which three-dimensional reconstructions of labeled perisynaptic astrocyte processes across groups could help to more conclusively explore this hypothesis. Alternatively, perisynaptic astrocyte processes could be scored from serial sections, such that one could validate that a labeled process is perisynaptic (Ventura and Harris, 1999). Lastly, as highlighted above, the possibility also remains that another PDZ scaffold might be meaningful for scaffolding Group II mGluRs in PAPs. The candidate Group II mGluR-interacting partners that are preferentially expressed in astrocytes include rhophilin, MAGI-3, PTPN13, and to a lesser extent, CAL and MUPP1. Interestingly, PTPN13 also contains an ERM-binding domain, which makes it a particularly intriguing candidate; however, based on the PDZ proteomic array data, PTPN13 appears to be an mGluR2-selective binding partner. Nevertheless, if loss of both NHERF proteins has no effect on Group II mGluR localization in PAPs, these additional astrocytic PDZ proteins could be explored as candidate astrocytic scaffolds controlling mGluR localization.

NHERF Proteins and Hydrocephaly: Evidence for an *in vivo* role of the NHERF proteins in CNS function

The NHERF-1 (N1) KO mice were originally developed by the laboratory of Ed Weinman at the University of Maryland via homologous recombination of exon 1 in the NHERF-1 gene and crossing onto a C57BL6/J background (JAX®) (Shenolikar et al., 2002). The initial reported phenotype of the N1 KO mice included phosphate wasting, decreased bone mineral content, increased urinary excretion of phosphate, and also defective cAMP-mediated regulation of the Nat+ and H+ exchanger, NHE3 (Shenolikar et al., 2002). Shenolikar et al. reported that some of the female N1 KO mice died from hydrocephaly, although this was not quantified and no additional CNS characterization was performed (Shenolikar et al., 2002). More quantitative findings regarding hydrocephalus in N1 KO mice on the C57BL6/J background have recently been reported, with this work additionally demonstrating that knockdown of NHERF-1 in zebrafish yields a hydrocephalus phenotype (Treat et al., 2016). Of note, studies comparing NHERF-1, NHERF-2, and NHERF-1/-2 knockout have been successfully performed with no reports of hydrocephalus, although these mice were on a distinct background (FVB/N) (Singh et al., 2009). It is quite possible that certain backgrounds are better-suited to generation of a NHERF-1/-2 null state and would help to determine to what extent NHERF-1/-2 might have overlapping functions.

Extending some of these initial observations regarding the role of NHERFs in the periphery to a CNS-focused characterization, we also observed a hydrocephaly phenotype in the N1 KO mice, which together with the observed ventriculomegaly, support the notion that N1 KO mice are more susceptible to hydrocephaly. As shown in Figure 7, more than 30% of male N1 KO mice developed severe hydrocephaly that resulted in either premature death or required euthanasia. No hydrocephaly was observed in corresponding WT or heterozygous mice that were born from the observed litters. Additionally, some female N1 KO mice also had hydrocephaly, but as we primarily used males for our studies, the effect in the females was not quantified. However, it should be pointed out that additional N1 KO mice have been reported, with no obvious signs of hydrocephaly or survival issues (Morales et al., 2004). Interestingly, these N1 KO mice are also on background C57BL6/J, but were generated via a retroviral gene trapping method to target exons 1–4 of NHERF-1, whereas the N1 KO mice utilized in our studies were generated via a neomycin insertion into exon 1 of NHERF-1. Thus, it is possible that the differences in the methods used to disrupt the NHERF-1 gene may be meaningful for the phenotype. It remains to be determined whether loss of NHERF-2 confers susceptibility to hydrocephaly, as ventriculomegaly was also observed in the N2 KO mice. Given that a putative and possibly functional NHERF-2 splice variant is upregulated in the N2 KO mice, this question would be best discerned in a model system in which all NHERF-2 splice variants were deleted and represent a question for future investigations.

It seems unlikely that NHERF interactions with Group II mGluRs bear any causal relationship to the development of hydrocephaly. No hydrocephaly phenotype has been reported in Group II mGluR knockout mice lacking either mGluR2, mGluR3 or both receptors (Linden et al., 2005, Lyon et al., 2008). Instead, the hydrocephaly phenotype may result from the role that has been attributed to NHERF-1 in the organization of the primary cilia (Francis et al., 2011), since deficits in motile and/or primary cilia have been shown to lead to hydrocephaly in mouse models (Ibanez-Tallon et al., 2004, Banizs et al., 2005, Davis et al., 2007, Tissir et al., 2010, Friedland-Little et al., 2011, Carter et al., 2012). This idea has been further developed in recent studies demonstrating that NHERF-1 can regulate planar cell polarity (PCP) via interaction with PCP core genes such as Frizzled and Vangl (Treat et al., 2016). Thus, PCP defects in ependymal cells lacking NHERF-1 may lead to deficiencies in ciliogenesis, resulting in perturbations in cerebrospinal fluid dynamics. These findings highlight an important role for NHERF-1 in the control of fluid homeostasis in the CNS and should be further explored in the future. It remains to be determined if NHERF-2 deficient mice are susceptible to hydrocephaly. The ventriculomegaly observed in the present study is supportive of this notion, but no obvious phenotype was observed. Thus, a more thorough study of N2 KO mice should be done in order to ascertain if N2 KO mice are also at risk for developing hydrocephaly.

Concluding Remarks

The studies described here identify NHERF-1 and NHERF-2 as novel interacting partners for Group II mGluRs and shed light on the physiological significance of scaffold protein interactions with glutamate receptors, ultimately enhancing our understanding of the

molecular mechanisms underlying both normal regulation and potential dysregulation of glutamatergic neurotransmission.

Acknowledgments

The authors thank Songbai Lin for assistance with primer design for the NHERF-2 KO mice, William Watkins for assistance with managing the NHERF-1 and NHERF-2 mouse colonies, Christopher Makinson for guidance on DNA extraction from mouse tails and genotyping, the lab of Tom Kukar lab for the use of their LI-COR for Western blot analyses, Meriem Gaval and Meagan Ward-Jenkins for assistance with dissections. Many personnel within the lab of Yoland Smith lab were instrumental in the electron microscopy studies, including Caroline Bolarinwa for assistance with the vibratome serial sectioning of the tissue, Susan Jenkins for guidance with the LM and EM reactions, and Jeff Pare for performing the ultracutting and assistance with the electron microscope. This work was supported by the National Institutes of Health (F31-MH086186 to SLR-M and R01-NS055179 to RAH).

Abbreviations

mGluR	metabotropic glutamate receptor
NHERF	Na+/H+ Exchanger Regulatory Factor
PDZ	postsynaptic density protein of 95 kDa (*P*SD95), *Drosophila* discs-large tumor suppressor A (*D*lgA), zona-occludens 1(*Z*o-1)
LY354740	(+)-2-aminobicyclo[3,1,0]hexane-2,6-dicarboxylic acid
WT	wild-type
N1 KO	NHERF-1 knockout
N2 KO	Full Length NHERF-2 knockout

References

Ardura JA, Friedman PA. Regulation of G protein-coupled receptor function by Na+/H+ exchange regulatory factors. Pharmacol Rev. 2011; 63:882–900. [PubMed: 21873413]

Aronica E, Gorter JA, Ijlst-Keizers H, Rozemuller AJ, Yankaya B, Leenstra S, Troost D. Expression and functional role of mGluR3 and mGluR5 in human astrocytes and glioma cells: opposite regulation of glutamate transporter proteins. Eur J Neurosci. 2003; 17:2106–2118. [PubMed: 12786977]

Banizs B, Pike MM, Millican CL, Ferguson WB, Komlosi P, Sheetz J, Bell PD, Schwiebert EM, Yoder BK. Dysfunctional cilia lead to altered ependyma and choroid plexus function, and result in the formation of hydrocephalus. Development. 2005; 132:5329–5339. [PubMed: 16284123]

Broere N, Hillesheim J, Tuo B, Jorna H, Houtsmuller AB, Shenolikar S, Weinman EJ, Donowitz M, Seidler U, de Jonge HR, Hogema BM. Cystic fibrosis transmembrane conductance regulator activation is reduced in the small intestine of Na+/H+ exchanger 3 regulatory factor 1 (NHERF-1)- but Not NHERF-2-deficient mice. J Biol Chem. 2007; 282:37575–37584. [PubMed: 17947234]

Bruno V, Battaglia G, Casabona G, Copani A, Caciagli F, Nicoletti F. Neuroprotection by glial metabotropic glutamate receptors is mediated by transforming growth factor-beta. J Neurosci. 1998; 18:9594–9600. [PubMed: 9822720]

Bruno V, Sureda FX, Storto M, Casabona G, Caruso A, Knopfel T, Kuhn R, Nicoletti F. The neuroprotective activity of group-II metabotropic glutamate receptors requires new protein synthesis and involves a glial-neuronal signaling. J Neurosci. 1997; 17:1891–1897. [PubMed: 9045718]

Cahoy JD, Emery B, Kaushal A, Foo LC, Zamanian JL, Christopherson KS, Xing Y, Lubischer JL, Krieg PA, Krupenko SA, Thompson WJ, Barres BA. A transcriptome database for astrocytes,

neurons, and oligodendrocytes: a new resource for understanding brain development and function. J Neurosci. 2008; 28:264–278. [PubMed: 18171944]

Cai Z, Saugstad JA, Sorensen SD, Ciombor KJ, Zhang C, Schaffhauser H, Hubalek F, Pohl J, Duvoisin RM, Conn PJ. Cyclic AMP-dependent protein kinase phosphorylates group III metabotropic glutamate receptors and inhibits their function as presynaptic receptors. J Neurochem. 2001; 78:756–766. [PubMed: 11520896]

Carter CS, Vogel TW, Zhang Q, Seo S, Swiderski RE, Moninger TO, Cassell MD, Thedens DR, Keppler-Noreuil KM, Nopoulos P, Nishimura DY, Searby CC, Bugge K, Sheffield VC. Abnormal development of NG2+PDGFR-alpha+ neural progenitor cells leads to neonatal hydrocephalus in a ciliopathy mouse model. Nat Med. 2012; 18:1797–1804. [PubMed: 23160237]

Ciccarelli R, D'Alimonte I, Ballerini P, D'Auro M, Nargi E, Buccella S, Di Iorio P, Bruno V, Nicoletti F, Caciagli F. Molecular signalling mediating the protective effect of A1 adenosine and mGlu3 metabotropic glutamate receptor activation against apoptosis by oxygen/glucose deprivation in cultured astrocytes. Mol Pharmacol. 2007; 71:1369–1380. [PubMed: 17293559]

Ciccarelli R, Sureda FX, Casabona G, Di Iorio P, Caruso A, Spinella F, Condorelli DF, Nicoletti F, Caciagli F. Opposite influence of the metabotropic glutamate receptor subtypes mGlu3 and -5 on astrocyte proliferation in culture. Glia. 1997; 21:390–398. [PubMed: 9419014]

D'Onofrio M, Cuomo L, Battaglia G, Ngomba RT, Storto M, Kingston AE, Orzi F, De Blasi A, Di Iorio P, Nicoletti F, Bruno V. Neuroprotection mediated by glial group-II metabotropic glutamate receptors requires the activation of the MAP kinase and the phosphatidylinositol-3-kinase pathways. J Neurochem. 2001; 78:435–445. [PubMed: 11483646]

Davis RE, Swiderski RE, Rahmouni K, Nishimura DY, Mullins RF, Agassandian K, Philp AR, Searby CC, Andrews MP, Thompson S, Berry CJ, Thedens DR, Yang B, Weiss RM, Cassell MD, Stone EM, Sheffield VC. A knockin mouse model of the Bardet-Biedl syndrome 1 M390R mutation has cilia defects, ventriculomegaly, retinopathy, and obesity. Proc Natl Acad Sci U S A. 2007; 104:19422–19427. [PubMed: 18032602]

Derouiche A, Anlauf E, Aumann G, Muhlstadt B, Lavialle M. Anatomical aspects of glia-synapse interaction: the perisynaptic glial sheath consists of a specialized astrocyte compartment. J Physiol Paris. 2002; 96:177–182. [PubMed: 12445894]

Derouiche A, Frotscher M. Peripheral astrocyte processes: monitoring by selective immunostaining for the actin-binding ERM proteins. Glia. 2001; 36:330–341. [PubMed: 11746770]

Diraddo JO, Miller EJ, Hathaway HA, Grajkowska E, Wroblewska B, Wolfe BB, Liotta DC, Wroblewski JT. A Real-Time Method for Measuring cAMP Production Modulated by Galphai/o-Coupled Metabotropic Glutamate Receptors. J Pharmacol Exp Ther. 2014

Doyle DA, Lee A, Lewis J, Kim E, Sheng M, MacKinnon R. Crystal structures of a complexed and peptide-free membrane protein-binding domain: molecular basis of peptide recognition by PDZ. Cell. 1996; 85:1067–1076. [PubMed: 8674113]

Durand D, Caruso C, Carniglia L, Lasaga M. Metabotropic glutamate receptor 3 activation prevents nitric oxide-induced death in cultured rat astrocytes. J Neurochem. 2010; 112:420–433. [PubMed: 20085613]

Enz R. Metabotropic glutamate receptors and interacting proteins: evolving drug targets. Curr Drug Targets. 2012; 13:145–156. [PubMed: 21777188]

Fam SR, Paquet M, Castleberry AM, Oller H, Lee CJ, Traynelis SF, Smith Y, Yun CC, Hall RA. P2Y1 receptor signaling is controlled by interaction with the PDZ scaffold NHERF-2. Proc Natl Acad Sci U S A. 2005; 102:8042–8047. [PubMed: 15901899]

Flajolet M, Rakhilin S, Wang H, Starkova N, Nuangchamnong N, Nairn AC, Greengard P. Protein phosphatase 2C binds selectively to and dephosphorylates metabotropic glutamate receptor 3. Proc Natl Acad Sci U S A. 2003; 100:16006–16011. [PubMed: 14663150]

Foo LC, Allen NJ, Bushong EA, Ventura PB, Chung WS, Zhou L, Cahoy JD, Daneman R, Zong H, Ellisman MH, Barres BA. Development of a method for the purification and culture of rodent astrocytes. Neuron. 2011; 71:799–811. [PubMed: 21903074]

Fotuhi M, Standaert DG, Testa CM, Penney JB Jr, Young AB. Differential expression of metabotropic glutamate receptors in the hippocampus and entorhinal cortex of the rat. Brain Res Mol Brain Res. 1994; 21:283–292. [PubMed: 8170352]

Fouassier L, Duan CY, Feranchak AP, Yun CH, Sutherland E, Simon F, Fitz JG, Doctor RB. Ezrin-radixin-moesin-binding phosphoprotein 50 is expressed at the apical membrane of rat liver epithelia. Hepatology. 2001; 33:166–176. [PubMed: 11124833]

Francis SS, Sfakianos J, Lo B, Mellman I. A hierarchy of signals regulates entry of membrane proteins into the ciliary membrane domain in epithelial cells. J Cell Biol. 2011; 193:219–233. [PubMed: 21444686]

Friedland-Little JM, Hoffmann AD, Ocbina PJ, Peterson MA, Bosman JD, Chen Y, Cheng SY, Anderson KV, Moskowitz IP. A novel murine allele of Intraflagellar Transport Protein 172 causes a syndrome including VACTERL-like features with hydrocephalus. Hum Mol Genet. 2011; 20:3725–3737. [PubMed: 21653639]

He J, Bellini M, Inuzuka H, Xu J, Xiong Y, Yang X, Castleberry AM, Hall RA. Proteomic analysis of beta 1-adrenergic receptor interactions with PDZ scaffold proteins. J Biol Chem. 2006; 281:2820–2827. [PubMed: 16316992]

Hirbec H, Perestenko O, Nishimune A, Meyer G, Nakanishi S, Henley JM, Dev KK. The PDZ proteins PICK1, GRIP, and syntenin bind multiple glutamate receptor subtypes. Analysis of PDZ binding motifs. J Biol Chem. 2002; 277:15221–15224. [PubMed: 11891216]

Hubert GW, Smith Y. Age-related changes in the expression of axonal and glial group I metabotropic glutamate receptor in the rat substantia nigra pars reticulata. J Comp Neurol. 2004; 475:95–106. [PubMed: 15176087]

Iacovelli L, Molinaro G, Battaglia G, Motolese M, Di Menna L, Alfiero M, Blahos J, Matrisciano F, Corsi M, Corti C, Bruno V, De Blasi A, Nicoletti F. Regulation of group II metabotropic glutamate receptors by G protein-coupled receptor kinases: mGlu2 receptors are resistant to homologous desensitization. Mol Pharmacol. 2009; 75:991–1003. [PubMed: 19164443]

Ibanez-Tallon I, Pagenstecher A, Fliegauf M, Olbrich H, Kispert A, Ketelsen UP, North A, Heintz N, Omran H. Dysfunction of axonemal dynein heavy chain Mdnah5 inhibits ependymal flow and reveals a novel mechanism for hydrocephalus formation. Hum Mol Genet. 2004; 13:2133–2141. [PubMed: 15269178]

Ivarsson Y. Plasticity of PDZ domains in ligand recognition and signaling. FEBS Lett. 2012; 586:2638–2647. [PubMed: 22576124]

Kitano J, Kimura K, Yamazaki Y, Soda T, Shigemoto R, Nakajima Y, Nakanishi S. Tamalin, a PDZ domain-containing protein, links a protein complex formation of group 1 metabotropic glutamate receptors and the guanine nucleotide exchange factor cytohesins. J Neurosci. 2002; 22:1280–1289. [PubMed: 11850456]

Lamprecht G, Weinman EJ, Yun CH. The role of NHERF and E3KARP in the cAMP-mediated inhibition of NHE3. J Biol Chem. 1998; 273:29972–29978. [PubMed: 9792717]

Lavialle M, Aumann G, Anlauf E, Prols F, Arpin M, Derouiche A. Structural plasticity of perisynaptic astrocyte processes involves ezrin and metabotropic glutamate receptors. Proc Natl Acad Sci U S A. 2011; 108:12915–12919. [PubMed: 21753079]

Linden AM, Shannon H, Baez M, Yu JL, Koester A, Schoepp DD. Anxiolytic-like activity of the mGLU2/3 receptor agonist LY354740 in the elevated plus maze test is disrupted in metabotropic glutamate receptor 2 and 3 knock-out mice. Psychopharmacology (Berl). 2005; 179:284–291. [PubMed: 15619115]

Lyon L, Kew JN, Corti C, Harrison PJ, Burnet PW. Altered hippocampal expression of glutamate receptors and transporters in GRM2 and GRM3 knockout mice. Synapse. 2008; 62:842–850. [PubMed: 18720515]

McCarthy KD, de Vellis J. Preparation of separate astroglial and oligodendroglial cell cultures from rat cerebral tissue. J Cell Biol. 1980; 85:890–902. [PubMed: 6248568]

Moldrich RX, Aprico K, Diwakarla S, O'Shea RD, Beart PM. Astrocyte mGlu(2/3)-mediated cAMP potentiation is calcium sensitive: studies in murine neuronal and astrocyte cultures. Neuropharmacology. 2002; 43:189–203. [PubMed: 12213273]

Morales FC, Takahashi Y, Kreimann EL, Georgescu MM. Ezrin-radixin-moesin (ERM)-binding phosphoprotein 50 organizes ERM proteins at the apical membrane of polarized epithelia. Proc Natl Acad Sci U S A. 2004; 101:17705–17710. [PubMed: 15591354]

Muly EC, Mania I, Guo JD, Rainnie DG. Group II metabotropic glutamate receptors in anxiety circuitry: correspondence of physiological response and subcellular distribution. J Comp Neurol. 2007; 505:682–700. [PubMed: 17948876]

Nicoletti F, Bruno V, Ngomba RT, Gradini R, Battaglia G. Metabotropic glutamate receptors as drug targets: what's new? Curr Opin Pharmacol. 2015; 20:89–94. [PubMed: 25506748]

Niethammer M, Valtschanoff JG, Kapoor TM, Allison DW, Weinberg RJ, Craig AM, Sheng M. CRIPT, a novel postsynaptic protein that binds to the third PDZ domain of PSD-95/SAP90. Neuron. 1998; 20:693–707. [PubMed: 9581762]

Ohishi H, Ogawa-Meguro R, Shigemoto R, Kaneko T, Nakanishi S, Mizuno N. Immunohistochemical localization of metabotropic glutamate receptors, mGluR2 and mGluR3, in rat cerebellar cortex. Neuron. 1994; 13:55–66. [PubMed: 8043281]

Pan Y, Weinman EJ, Dai JL. Na+/H+ exchanger regulatory factor 1 inhibits platelet-derived growth factor signaling in breast cancer cells. Breast Cancer Res. 2008; 10:R5. [PubMed: 18190691]

Paquet M, Asay MJ, Fam SR, Inuzuka H, Castleberry AM, Oller H, Smith Y, Yun CC, Traynelis SF, Hall RA. The PDZ scaffold NHERF-2 interacts with mGluR5 and regulates receptor activity. J Biol Chem. 2006a; 281:29949–29961. [PubMed: 16891310]

Paquet M, Kuwajima M, Yun CC, Smith Y, Hall RA. Astrocytic and neuronal localization of the scaffold protein Na+/H+ exchanger regulatory factor 2 (NHERF-2) in mouse brain. J Comp Neurol. 2006b; 494:752–762. [PubMed: 16374813]

Patil ST, Zhang L, Martenyi F, Lowe SL, Jackson KA, Andreev BV, Avedisova AS, Bardenstein LM, Gurovich IY, Morozova MA, Mosolov SN, Neznanov NG, Reznik AM, Smulevich AB, Tochilov VA, Johnson BG, Monn JA, Schoepp DD. Activation of mGlu2/3 receptors as a new approach to treat schizophrenia: a randomized Phase 2 clinical trial. Nat Med. 2007; 13:1102–1107. [PubMed: 17767166]

Peters, A., Palay, SL., Webster, HF. The Fine Structure of the Nervous System: Neurons and Their Supporting Cells. New York: Oxford University Press; 1991.

Petralia RS, Wang YX, Niedzielski AS, Wenthold RJ. The metabotropic glutamate receptors, mGluR2 and mGluR3, show unique postsynaptic, presynaptic and glial localizations. Neuroscience. 1996; 71:949–976. [PubMed: 8684625]

Phillips T, Rees S, Augood S, Waldvogel H, Faull R, Svendsen C, Emson P. Localization of metabotropic glutamate receptor type 2 in the human brain. Neuroscience. 2000; 95:1139–1156. [PubMed: 10682721]

Ritter SL, Asay MJ, Paquet M, Paavola KJ, Reiff RE, Yun CC, Hall RA. GLAST stability and activity are enhanced by interaction with the PDZ scaffold NHERF-2. Neurosci Lett. 2011; 487:3–7. [PubMed: 20430067]

Ritter SL, Hall RA. Fine-tuning of GPCR activity by receptor-interacting proteins. Nature Reviews Molecular Cell Biology. 2009; 10:819–830. [PubMed: 19935667]

Schaffhauser H, Cai Z, Hubalek F, Macek TA, Pohl J, Murphy TJ, Conn PJ. cAMP-dependent protein kinase inhibits mGluR2 coupling to G-proteins by direct receptor phosphorylation. J Neurosci. 2000; 20:5663–5670. [PubMed: 10908604]

Schoepp DD, Johnson BG, Wright RA, Salhoff CR, Mayne NG, Wu S, Cockerman SL, Burnett JP, Belegaje R, Bleakman D, Monn JA. LY354740 is a potent and highly selective group II metabotropic glutamate receptor agonist in cells expressing human glutamate receptors. Neuropharmacology. 1997; 36:1–11. [PubMed: 9144636]

Seebahn A, Rose M, Enz R. RanBPM is expressed in synaptic layers of the mammalian retina and binds to metabotropic glutamate receptors. FEBS Lett. 2008; 582:2453–2457. [PubMed: 18555800]

Sheng M, Sala C. PDZ domains and the organization of supramolecular complexes. Annu Rev Neurosci. 2001; 24:1–29. [PubMed: 11283303]

Shenolikar S, Voltz JW, Minkoff CM, Wade JB, Weinman EJ. Targeted disruption of the mouse NHERF-1 gene promotes internalization of proximal tubule sodium-phosphate cotransporter type IIa and renal phosphate wasting. Proc Natl Acad Sci U S A. 2002; 99:11470–11475. [PubMed: 12169661]

Singh AK, Riederer B, Krabbenhoft A, Rausch B, Bonhagen J, Lehmann U, de Jonge HR, Donowitz M, Yun C, Weinman EJ, Kocher O, Hogema BM, Seidler U. Differential roles of NHERF1, NHERF2, and PDZK1 in regulating CFTR-mediated intestinal anion secretion in mice. J Clin Invest. 2009; 119:540–550. [PubMed: 19221439]

Sun W, McConnell E, Pare JF, Xu Q, Chen M, Peng W, Lovatt D, Han X, Smith Y, Nedergaard M. Glutamate-dependent neuroglial calcium signaling differs between young and adult brain. Science. 2013; 339:197–200. [PubMed: 23307741]

Takahashi Y, Morales FC, Kreimann EL, Georgescu MM. PTEN tumor suppressor associates with NHERF proteins to attenuate PDGF receptor signaling. EMBO J. 2006; 25:910–920. [PubMed: 16456542]

Tamaru Y, Nomura S, Mizuno N, Shigemoto R. Distribution of metabotropic glutamate receptor mGluR3 in the mouse CNS: differential location relative to pre- and postsynaptic sites. Neuroscience. 2001; 106:481–503. [PubMed: 11591452]

Tanabe Y, Nomura A, Masu M, Shigemoto R, Mizuno N, Nakanishi S. Signal transduction, pharmacological properties, and expression patterns of two rat metabotropic glutamate receptors, mGluR3 and mGluR4. J Neurosci. 1993; 13:1372–1378. [PubMed: 8463825]

Testa CM, Standaert DG, Young AB, Penney JB Jr. Metabotropic glutamate receptor mRNA expression in the basal ganglia of the rat. J Neurosci. 1994; 14:3005–3018. [PubMed: 8182455]

Tissir F, Qu Y, Montcouquiol M, Zhou L, Komatsu K, Shi D, Fujimori T, Labeau J, Tyteca D, Courtoy P, Poumay Y, Uemura T, Goffinet AM. Lack of cadherins Celsr2 and Celsr3 impairs ependymal ciliogenesis, leading to fatal hydrocephalus. Nat Neurosci. 2010; 13:700–707. [PubMed: 20473291]

Treat AC, Wheeler DS, Stolz DB, Tsang M, Friedman PA, Romero G. The PDZ Protein Na+/H+ Exchanger Regulatory Factor-1 (NHERF1) Regulates Planar Cell Polarity and Motile Cilia Organization. PLoS One. 2016; 11:e0153144. [PubMed: 27055101]

Ventura R, Harris KM. Three-dimensional relationships between hippocampal synapses and astrocytes. J Neurosci. 1999; 19:6897–6906. [PubMed: 10436047]

Vinson PN, Conn PJ. Metabotropic glutamate receptors as therapeutic targets for schizophrenia. Neuropharmacology. 2012; 62:1461–1472. [PubMed: 21620876]

Wroblewska B, Wegorzewska IN, Bzdega T, Neale JH. Type 2 metabotropic glutamate receptor (mGluR2) fails to negatively couple to cGMP in stably transfected cells. Neurochem Int. 2011; 58:176–179. [PubMed: 21115084]

Wroblewska B, Wroblewski JT, Pshenichkin S, Surin A, Sullivan SE, Neale JH. N-acetylaspartylglutamate selectively activates mGluR3 receptors in transfected cells. J Neurochem. 1997; 69:174–181. [PubMed: 9202308]

Yun CC, Chen Y, Lang F. Glucocorticoid activation of Na(+)/H(+) exchanger isoform 3 revisited. The roles of SGK1 and NHERF2. J Biol Chem. 2002; 277:7676–7683. [PubMed: 11751930]

Yun CH, Lamprecht G, Forster DV, Sidor A. NHE3 kinase A regulatory protein E3KARP binds the epithelial brush border Na+/H+ exchanger NHE3 and the cytoskeletal protein ezrin. J Biol Chem. 1998; 273:25856–25863. [PubMed: 9748260]

Highlights

- NHERF-1 & -2 are novel interacting partners of mGluR2 and mGluR3
- NHERF-1 & -2 bind to conserved C-terminal motifs on mGluR2/3
- Removal of the PDZ-binding motif enhances mGluR2 signaling
- Subcellular localization of mGluR2/3 is altered in NHERF-2 knockout mice.

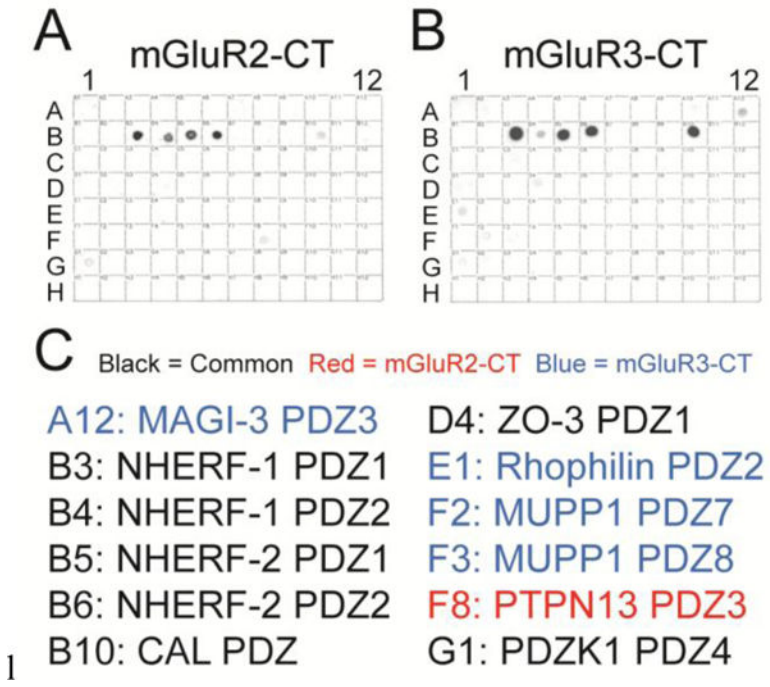

Figure 1. The C-termini of mGluR2 and mGluR3 bind selectively to NHERF PDZ domains

A–B) The C-termini (CT) of mGluR2 (**A**) and mGluR3 (**B**) were screened for binding to an array of 96 distinct PDZ domains. The PDZ domains of NHERF-1 and NHERF-2 were the strongest hits for mGluR2 (**A**) and mGluR3 (**B**). A complete list of the PDZ proteins on this array has been described previously (He et al., 2006). The data shown here are representative of three independent experiments. **C)** A summary of the PDZ domains found to interact with either mGluR2/3-CT (black), mGluR2-CT alone (red), or mGluR3-CT alone (blue).

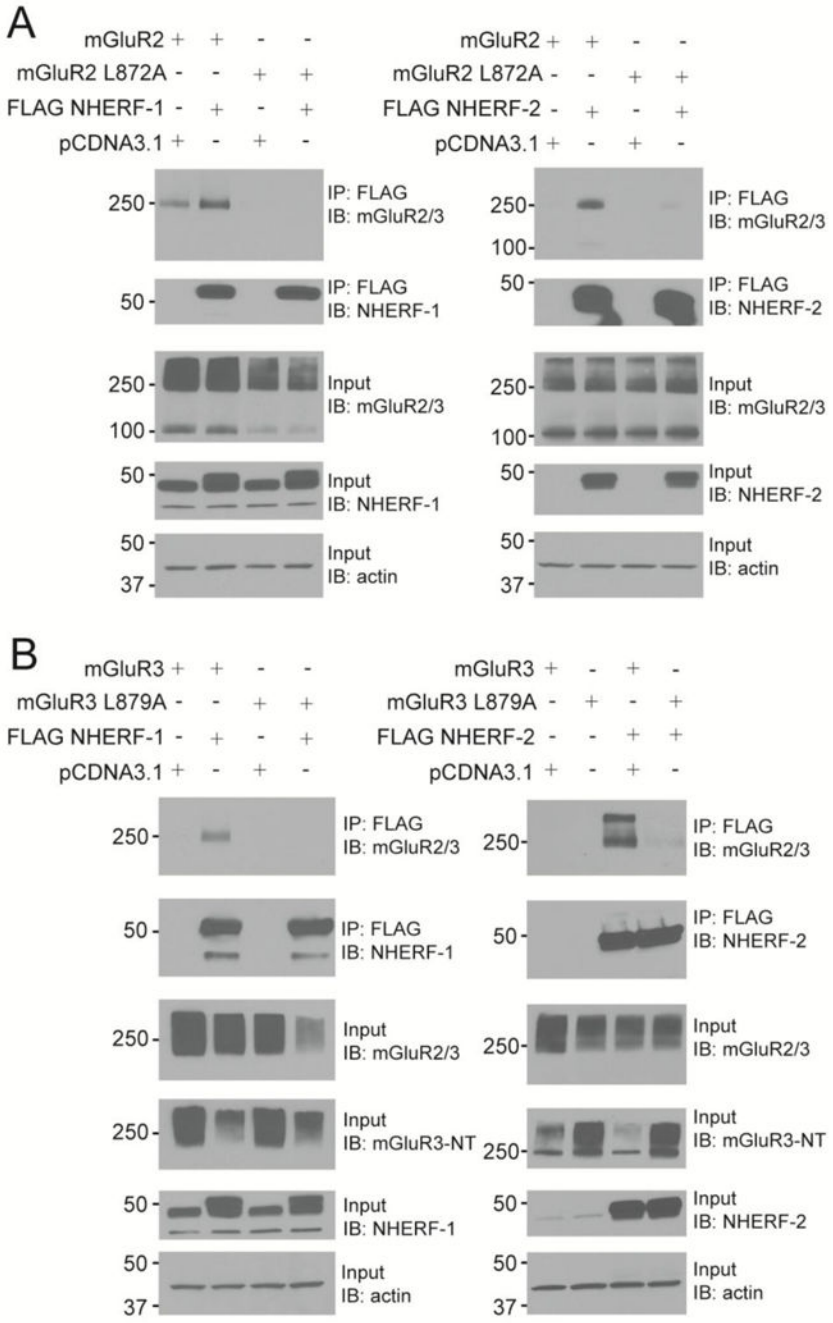

Figure 2. Group II mGluRs associate with NHERF-1 or NHERF-2 in a cellular context and require the last amino acid

HEK293T cells were transiently transfected with mock pcDNA3.1, mGluR2, mGluR2 L872A, mGluR3, mGluR3 L879A, or FLAG NHERF-1 or FLAG-NHERF-2 cDNAs. Robust immunoprecipitation of FLAG-tagged NHERF-1 **(left panel, A and B)** or NHERF-2 **(right panel, A and B)** was achieved in all experiments and subsequently examined for co-immunoprecipitation of mGluR2 or mGluR2 L872A **(A)** and mGluR3 or mGluR3 L879A **(B)** relative to background co-precipitation signal alone. **A)** Mutation of the last amino acid

of mGluR2 was sufficient to disrupt NHERF-1 association (left, top panel, lanes 2 vs. 4). This lack of association could not be explained by differences in mGluR2 and mutant mGluR2 L872A expression, as similar total levels of protein were used in the study as revealed by comparison to actin labeling (left, bottom panel). It should be noted that the mGluR2/3 antibody detects the C-terminus of mGluR2 and mGluR3; thus, the mutation reduces detection of mGluR2 or mGluR3. Likewise, mutation of the last amino acid of mGluR2 was also sufficient to disrupt NHERF-2 association (right, top panel, lane 2 vs. 4). Similar results were obtained in 2–5 independent experiments. **B)** Mutation of the last amino acid of mGluR3 was sufficient to disrupt NHERF-1 association (left, top panels, lanes 2 vs. 4, detecting mGluR3 with both a C-terminal (IB: mGluR2/3) and N-terminal (IB: mGluR3-NT) antibody). This lack of association could not be explained by differences in mGluR3 and mutant mGluR3 L879A expression, as similar total levels of protein were expressed in the study as revealed by comparison to actin labeling (left, bottom panel) and comparable detection of mGluR3 input with the N-terminal antibody. Likewise, mutation of the last amino acid of mGluR3 was also sufficient to disrupt NHERF-2 association (right, top 2 panels, lane 3 vs. 4). Similar results were obtained in 2–5 independent experiments.

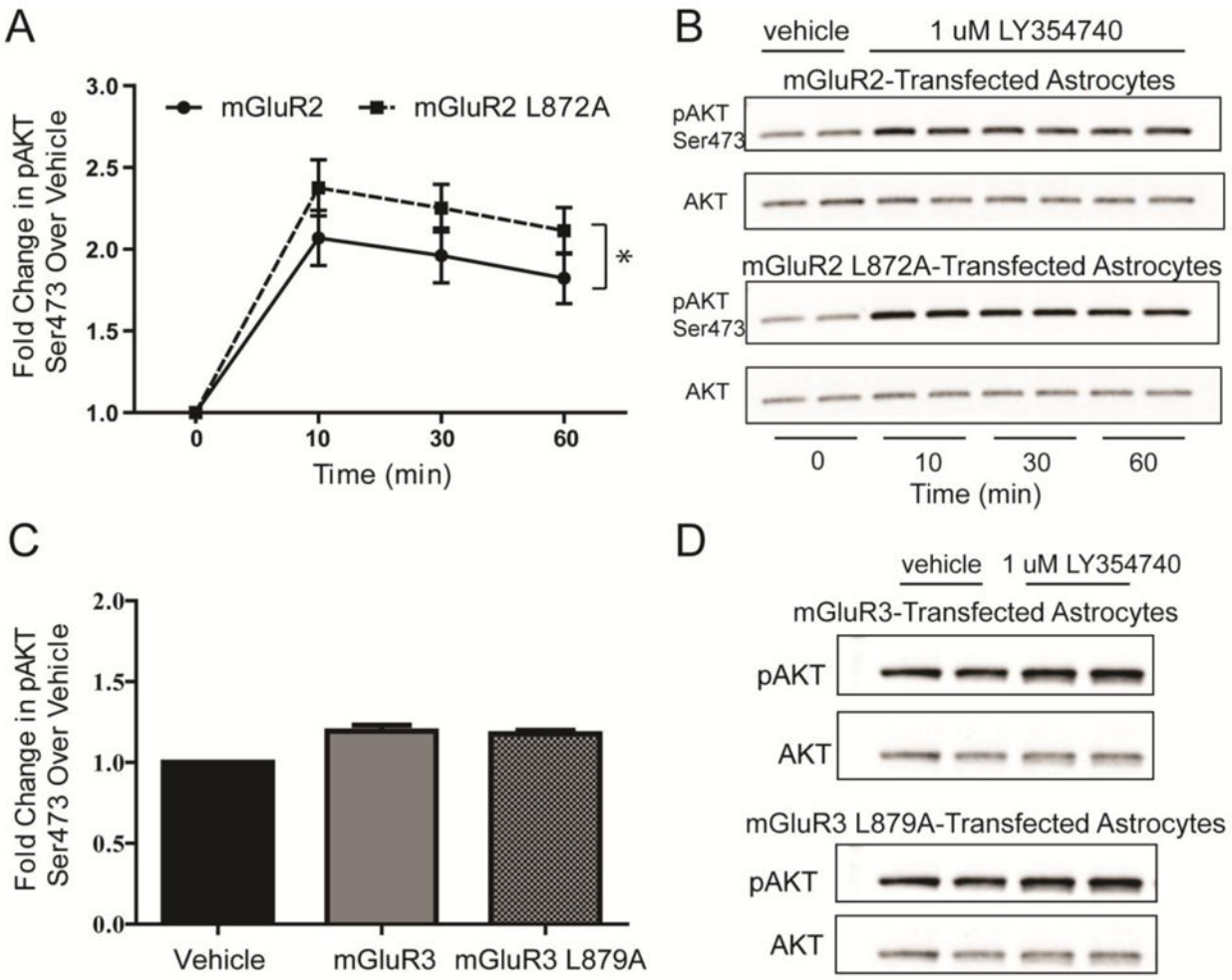

Figure 3. Examination of the effects of mutation of the Group II mGluR-PDZ-interacting motif on AKT signaling

Mouse cortical astrocyte cultures expressing mGluR2 or mGluR2 L872A **(A and B)** and mGluR3 or mGluR3 L879A **(C and D)** were stimulated with either vehicle (media) or 1 μM LY354740 for designated periods of time. Astrocyte lysates were simultaneously probed for pAKT (Ser473) and total AKT. Graphs depict average fold change ± S.E.M. of normalized pAKT/AKT integrated densities over vehicle treatment. **A)** Analysis of mGluR2- and L872A-mediated AKT signaling via two-way ANOVA revealed an overall significant effect of receptor on signaling (n = 8, p = 0.0298, *). Enhanced mGluR2 L872A signaling was observed in 6 out of 8 individual experiments. **B)** Representative immunoblot showing the agonist-dependent activation of pAKT. **C)** A student's t-test revealed there was no significant difference between mGluR3- and L879A-mediated AKT signaling (n = 8). **D)** Representative immunoblot showing the comparably small agonist-dependent activation of pAKT in mGluR3-expressing astrocytes.

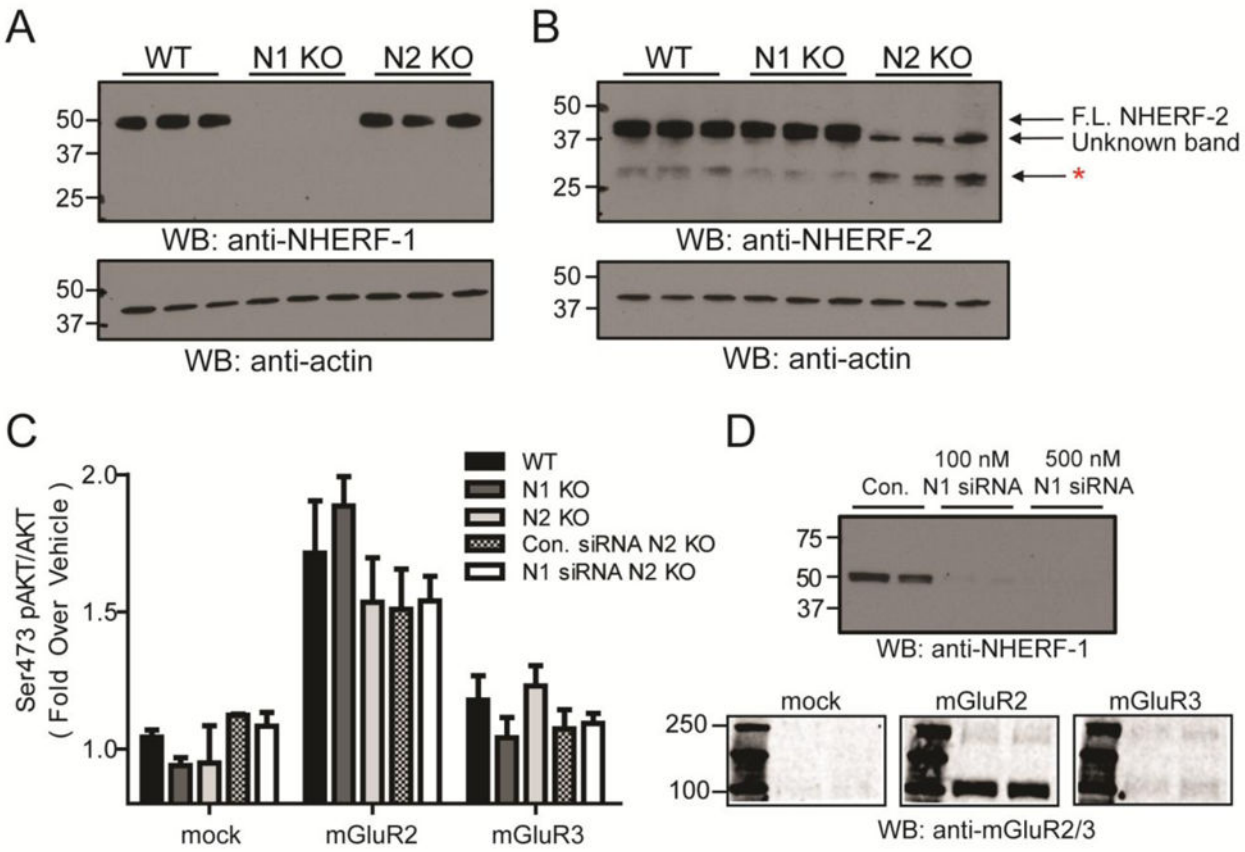

Figure 4. Examination of mGluR2 and mGluR3 signaling in cultured astrocytes devoid of NHERF proteins

A) Full length NHERF-1 is absent in brain lysates from N1 KO animals and its levels are unchanged in WT and N2 KO mice. Similarly, full-length NHERF-2 is also absent in brain lysates from N2 KO mice and its levels are unchanged in WT and N1 KO mice **(B)**. However, a presumed NHERF-2 splice variant (asterisk) that is predicted to be 24.5 kDa, and runs at approximately 27 kDa, appears upregulated in N2 KO mice and its levels are slightly decreased in N1 KO mice, relative to WT mouse brain samples. The other band detected with the NHERF-2 antibody is unknown; it may reflect a non-specific band as this is a polyclonal antibody that is not affinity purified, or alternatively it may indicate another NHERF-2 splice variant. **C-D)** Cortical astrocytes were prepared from WT, N1 KO, N2 KO, or N2 KO cultures treated with 250 nM control siRNA or NHERF-1 siRNA. Cultures were then transfected with mock (pcDNA3.1), mGluR2, or mGluR3 cDNAs and after 24 hours of expression and 3 hour serum starvation, were stimulated with either vehicle or 1 μM LY354740 for 10 min. Graphs depict normalized pAKT/AKT integrated densities ± S.E.M. Analysis of the activation of Ser473 AKT **(C)**. Analysis with Two-Way ANOVA revealed no significant effect of genotype, $p = 0.86$, n.s. However, a significant effect of receptor was observed, in accordance with the differential ability of mock-, mGluR2-, or mGluR3-transfected astrocytes to activate AKT, $p < 0.0001$, ***. These data are representative of 3–5 independent experiments per condition. **D)** Western blots characterizing the model system used in this study. Cultured astrocytes were treated with control siRNA, or 100 nM or 500

nM of NHERF-1 siRNA and were probed for NHERF-1 three days following transfection, revealing a dose-dependent knock-down of NHERF-1 with siRNA treatment (top panel). Demonstration of successful transfection of mGluR2 and mGluR3 of cultured astrocytes, as measured by Western blot analysis with an mGluR2/3 C-terminal antibody (bottom panels; lane 1, molecular weight ladder; lanes 2 and 3, lysates from astrocyte cultures from either mock-transfected, mGluR2-transfected, or mGluR3-transfected conditions). Note that the signal for mGluR3 is relatively weak in comparison to mGluR2, despite equal transfection of mGluR2 and mGluR3 plasmids.

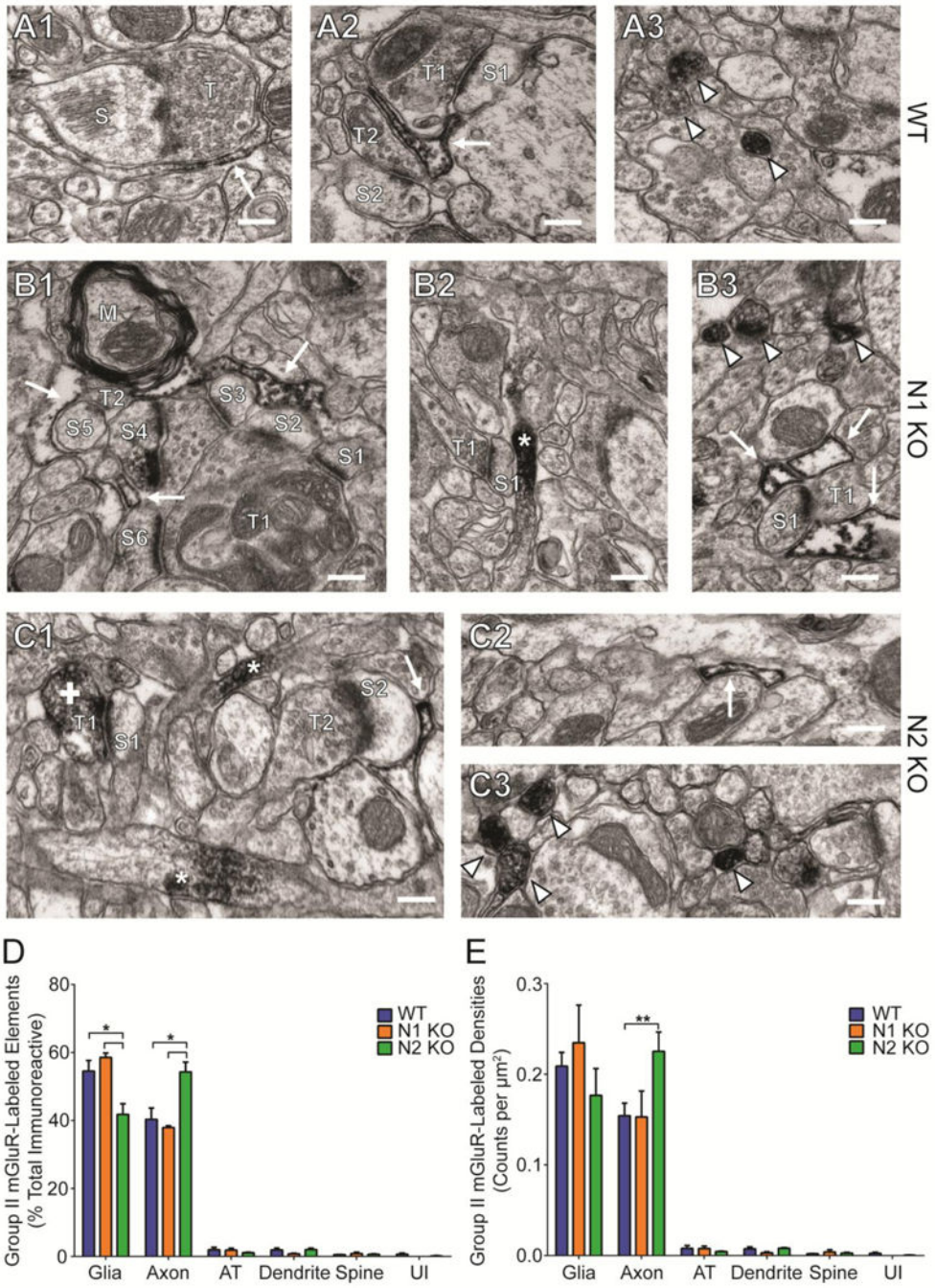

Figure 5. Distribution of Group II mGluR labeling in WT, N1 KO, and N2 KO mouse cortex

A) Examples of Group II mGluR labeling in WT mice. **A1)** Labeling was often observed in perisynaptic glial processes (arrows) that were positioned near asymmetric axospinous synapses. **A2)** Labeled glial processes also contacted multiple synapses in some cases; shown here is a labeled glial process physically contacting two different asymmetric synapses (arrow). **A3)** Cross-sections of pre-terminal, unmyelinated axons were also commonly observed, as denoted by arrowheads. However, post-synaptic labeling was rarely seen. **B)** Examples of Group II mGluR labeling in N1 KO mice. **B1)** Glial Group II mGluR

labeling was also commonly observed. Shown is a labeled glial process (arrow) that surrounds four separate asymmetric axospinous synapses. Interestingly, the labeled glial process also comes in contact with a myelinated axon (M), which is not labeled. Two additional Group II mGluR-labeled processes are present (arrows). **B2)** An immunopositive axon passes near an asymmetric axospinous synapse. **B3)** Additional examples of labeled axons cut in transverse (arrowheads) and immunopositive glial process (arrows). **C)** Increased immunolabeled unmyelinated axons were observed in N2 KO mice, although the quantification of glial labeling was unchanged from WT and N1 KO mice. **C1)** Examples of axonal (arrowheads, transverse; asterisks, parallel), glial (arrow), and axon terminal (cross) labeling are shown here. **C2)** An example of a labeled glial element (arrow) that is not by an asymmetric synapse. **C3)** A field of axons is shown in which many of the axons are labeled for Group II mGluRs (arrowheads). Scale bar is 0.2 μm. Abbreviations used: T is for terminal, S is for spine. **D,E**) Histograms showing the relative distribution or density (counts/area) of Group II mGluR immunoreactive elements in the cortex of WT, N1 KO, or N2 KO mice. **D)** The relative distribution of Group II mGluR labeling was quantified across various elements in the cortex. Data are expressed as percent total of immunoreactive elements (mean ± S.E.M.). The predominant elements labeled for all genotypes were glia and pre-terminal, unmyelinated axons (Un. Axon), with infrequent labeling observed in axon terminals (AT), dendrites, and spines. A small fraction of labeling was classified as unidentified (UI). WT and N1 KO mice had significantly more glia labeling of Group II mGluRs, while N2 KO mice had significantly more axonal labeling of Group II mGluRs, reflecting a shift in the distribution. (One-way ANOVA Glia: $p = 0.0223$; One-way ANOVA Axons: $p = 0.0238$). **E)** More Group II mGluR immunoreactive axons were counted in N2 KO mice than in WT or N1 KO mice, while similar densities of glial profiles were observed across all three genotypes. Data are expressed as density per μm^2 (mean ± S.E.M.) of labeled elements. A total of 304 (WT), 155 (N1 KO), and 150 (N2 KO) micrographs were examined representing approximately 4496 μm^2 (WT, n = 6), 2292 μm^2 (N1 KO, n = 3), and 2219 μm^2 (N2 KO, n = 3) tissue, respectively. Analysis of Two-Way ANOVA with Bonferonni post-hoc tests for multiple comparisons reveals that N2 KO mice have a higher density of labeled axons in comparison to WT or N1 KO mice (** $p < 0.01$).

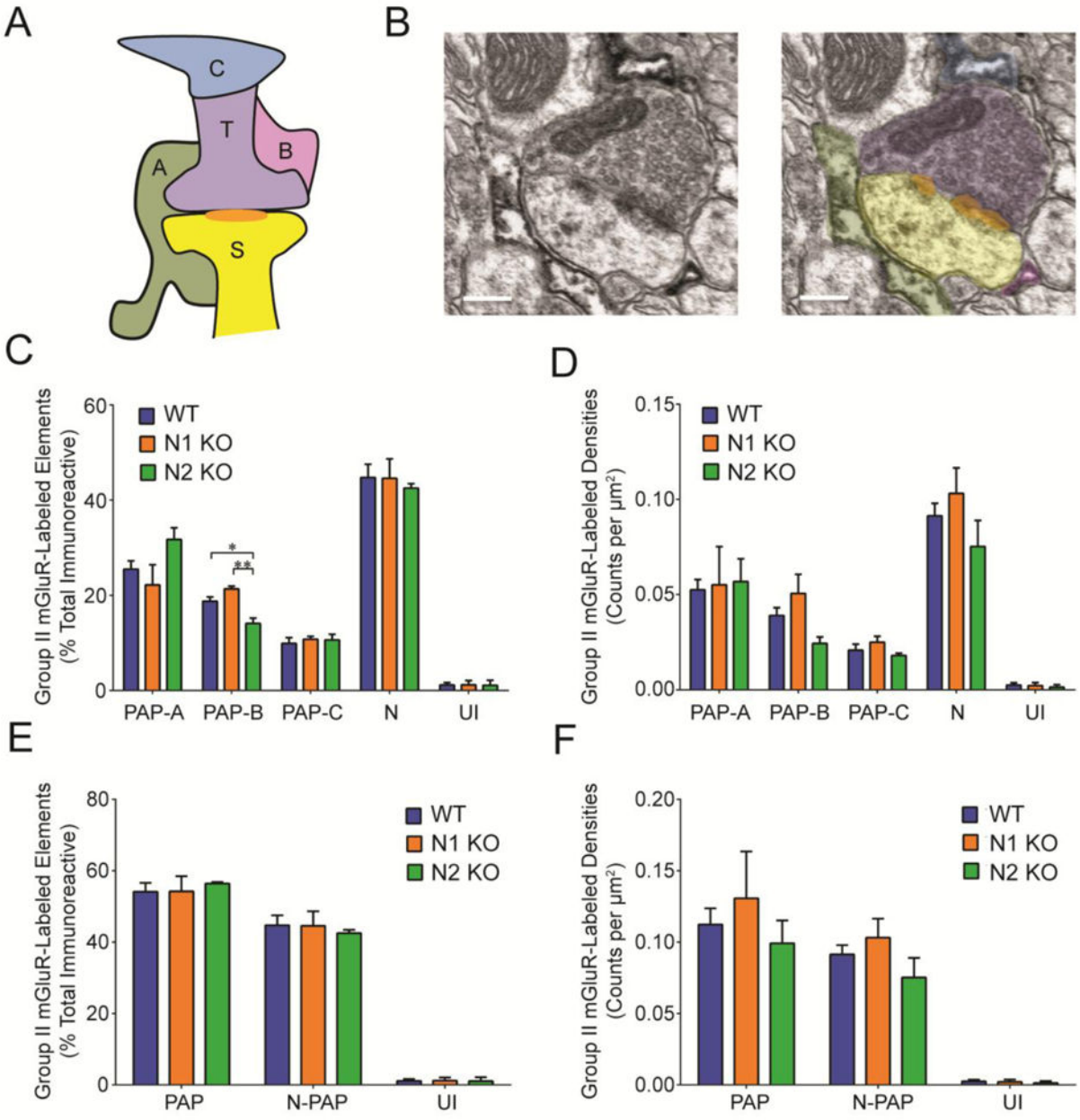

Figure 6. Distribution of Group II mGluR-immunoreactivity in perisynaptic astrocyte processes (PAPs) across WT, N1 KO, and N2 KO mice

A) Group II mGluR-immunopositive astrocyte compartments were subdivided into perisynaptic classifications based on their coverage of the synapse (S, spine; T, terminal; A, B & C, perisynaptic astrocyte processes type A, B & C, as defined in the Methods section). **B)** Electron micrographs showing the identified elements in accordance with the color classification in **(A)**. **C)** Relative distribution of Group II mGluR-immunoreactivity across perisynaptic astrocyte processes (PAP). Data are expressed as percent total of immunoreactive element (mean ± S.E.M.). One-way ANOVA tests with Tukey post-hoc tests for multiple comparisons reveal that N2 KO mice have significantly less Group II mGluR-labeled PAP-B relative to WT or N1 KO mice ($p < 0.0036$). **D)** Data are expressed as density

per μm^2 (mean ± S.E.M.) of labeled elements. A total of 304 (WT), 155 (N1 KO), and 150 (N2 KO) micrographs were examined representing approximately 4496 μm^2 (WT, n = 6), 2292 μm^2 (N1 KO, n = 3), and 2219 μm^2 (N2 KO, n = 3) tissue, respectively. No significant differences in PAP or non-PAP densities were observed across genotypes (Two-way ANOVA, post hoc Bonferonni test for multiple comparisons). **E)** Collapse of PAP-A, B, C relative distribution shown in **(C)**. No significant differences were observed across genotypes, although more Group II mGluR labeling was consistently observed across all genotypes, relative to non-PAP or unidentified (UI) labeling. **F)** Collapse of PAP-A, B, C mean densities shown in **(D)**. No significant differences were observed across genotypes.

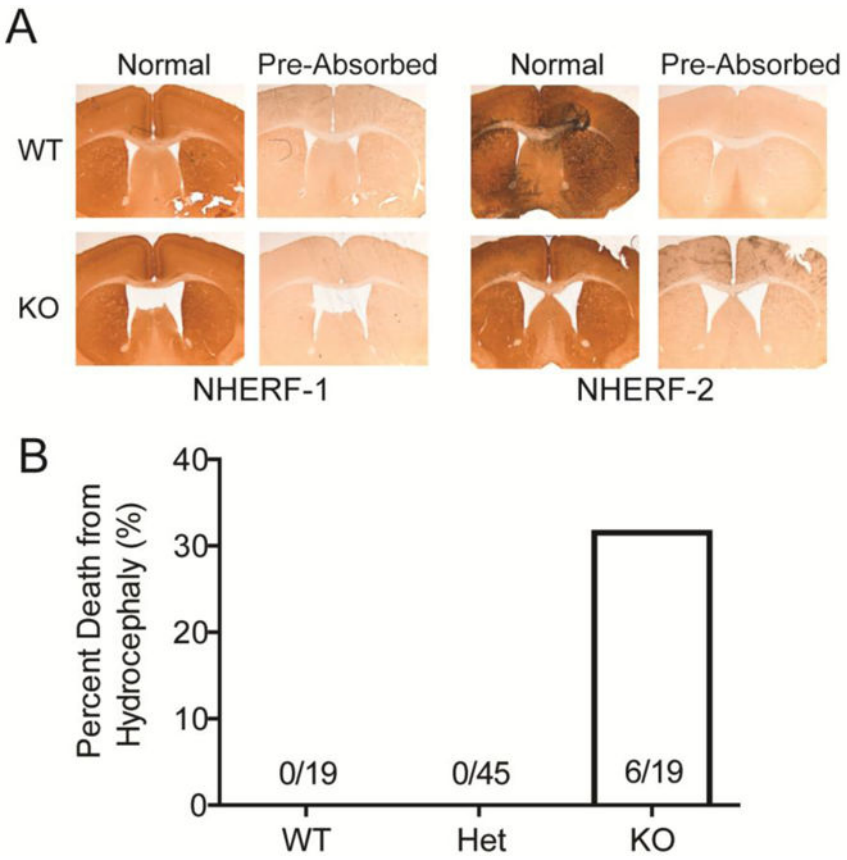

Figure 7. N1 KO and N2 KO mice display ventriculomegaly, accomapanied by a severe hydrocephaly phenotype in N1 KO mice

Light microscopy reactions with Group II mGluR antibody (Ab1553) were done in parallel with an mGluR2-CT peptide that was pre-absorbed with the Group II mGluR antibody. Note the absence of Group II mGluR signal in the peptide pre-absorbed conditions for all groups examined. **(A)** Interestingly, all N1 KO (n = 3) and N2 KO (n = 3) mice had enlarged ventricles relative to their littermate controls. Sections used in the staining were all selected from a similar plane. **B)** Percentage of surviving male wild-type (WT), heterozygous (Het), and N1 KO mice, as measured up to a 3.5 month time period. The hydrocephaly phenotype was denoted by a swollen head and appearance of sunken eyes, and confirmed via consultations with veterinary staff. Out of 19 N1 KO mice that were genotyped, 6 mice developed severe hydrocephaly and either died or were euthanized, while hydrocephaly was not observed in WT (19 out 19) or Het (45 out 45) mice. The phenotype generally presented between the first and second months of age. Those mice whose death was unclear were not included in this analysis. Hydrocephaly was also observed in female N1 KO mice, although this was not quantified due to the small sample number.